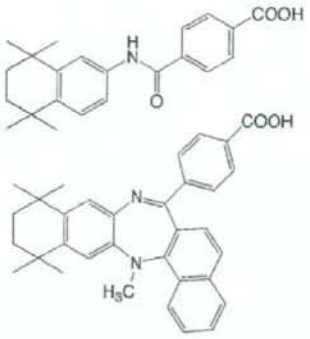

Chart 1. Am80 and LE540 (top and bottom).

CRABP-dependent retinoid-resistance will be avoided. Moreover, Am80 is much more stable than ATRA in the contexts of light, heat, and oxidation. In comparison, LE540 is an RAR antagonist, and its inhibition activity for Am80-induced HL-60 cell differentiation has been reported [22]. Targeting and the controlled release of these retinoids through micelle encapsulation will expand their therapeutic applications, especially when the target is solid tumor tissue for Am80.

Chemical-structure characteristics of Am80 and LE540 constitute the other reason for the selection. We use the hydrophobic frames of these retinoids to encapsulate the compounds into micelles. As compared with Am80, LE540 has bulkier hydrophobic moiety. Therefore, these two retinoids not only possess high therapeutic potential, but also benefit analysis on relations between the chemical structures of drugs and the corresponding encapsulation-release behaviors of the retinoids.

In this study, we perform encapsulation of Am80 and LE540 into micelles forming from PEG-poly(benzyl aspartate) block copolymers and analyze the retinoids' encapsulation behaviors and release rates. Am80 and LE540 are sufficiently hydrophobic in water for easy and efficient encapsulation into a polymeric micelle. However, Am80 is soluble in Dulbecco's phosphate buffered saline (D-PBS) and is rapidly released from a polymeric micelle. Therefore we have attempted to control the release rates by means of an addition of hydrophobic compounds interacting with Am80. This is a novel methodology for the control of drug-release rates from polymeric micelle carriers. Even though addition of oppositely charged hydrophobic compounds have been frequently used in traditional drug carriers such as microparticles, the first time application of this method for the polymeric micelle carriers is very important. The reason for the importance is that extremely stable drug encapsulation (e.g., 10^{-19} cm^2/s diffusion coefficient [23]) is required due to a very small micellar inner core such as 10 nm in diameter as a drug container.

2. Materials and methods

2.1. Materials and equipment

For the present study, α-methoxy-ω-amino poly(ethylene glycol) (MeO-PEG-NH_2) (Mw 5-kDa) was purchased from NOF Corp. (Tokyo, Japan). And β-benzyl L-aspartate was purchased from Kokusan Chemical (Tokyo, Japan). Triphosgene was obtained from Tokyo Chemical Industry Co., Ltd. (Tokyo, Japan) and used as received. β-Benzyl L-aspartate *N*-carboxyanhydride (BLA-NCA) was prepared from β-benzyl L-aspartate and triphosgene according to the conventional method [24]. DMF was distilled at a reduced pressure before use. All other reagents used were of reagent grade. ^{1}H-NMR measurements were carried out with a Varian Unity Inova NMR spectrometer (Varian Technologies Japan Ltd., Tokyo, Japan) at 400 MHz. A Spectra/Por 6 dialysis membrane (Spectrum Laboratories Inc., CA, USA) (1-kDa cut-off) was used for dialysis. An HPLC analysis was carried out with an HPLC system (PU-2080 plus pump; MX-2080-32 dynamic mixer; UV-2070 plus UV detector; and RI-2031 plus RI detector, Jasco Corp., Tokyo, Japan) equipped with a TSK-gel ODS-80Ts reverse-phased column (150 × 4.6 mm i.d., Tosoh Corp., Tokyo, Japan). Dynamic light scattering (DLS) measurements were performed in 1.0% (w/w) aqueous solutions at 25 °C with a DLS-7000 (Otsuka Electronic Co. Ltd., Osaka, Japan). Particle size distribution in terms of weight fractions was calculated using a non-negative least squares (NNLS) algorithm.

2.2. Synthesis of amphiphilic diblock copolymers

Polymers used for encapsulation of retinoids are composed of a PEG-poly(aspartic acid) (PEG-P(Asp)) main chain and pendant benzyl groups (Table 1). PEG-poly(benzyl L-aspartate) (PEG-PBLA) polymers **1** and **2** were prepared by ring-opening polymerization of BLA-NCA from a primary amino terminal of MeO-PEG-NH_2 [25]. The PEG-P(Asp (Bzl)$_x$) polymers **3**–**5** were obtained as follows: (1) complete removal of benzyl groups from PEG-PBLA [26], and (2) partial esterification of PEG-P(Asp) with benzyl bromide (BzlBr) [27].

2.2.1. Synthesis of PEG-*b*-poly(β-benzyl L-aspartate) (PEG-PBLA)

PEG-*b*-poly(β-benzyl L-aspartate) (PEG-PBLA) block copolymers were synthesized according to literature [25]. Amino-terminated poly (ethylene glycol) MeO-PEG-NH_2 as a macroinitiator was mixed with BLA-NCA in a dichloromethane–DMF mixed solvent (9:1 v/v), and this mixture was stirred at 35 °C for 17 h under a nitrogen atmosphere. The reaction mixture was dropwisely added into diethyl ether cooled in ice. The resulting precipitate was collected by filtration, washed with diethyl ether, and dried under a reduced pressure. The degree of polymerization (DP, i.e., the average unit number of polymer chain) of the PBLA block was determined by ^{1}H-NMR spectroscopy in chloroform-*d*. The determination was based on an integration ratio between the proton assigned to the methylene of PEG (3.8–3.4 ppm) and the benzyl methylene of PBLA (5.2–4.9 ppm). The polymers **1** and **2** were estimated to be 24 and 28, respectively.

Table 1
Synthesis of PEG-P(Asp (Bzl)$_x$) block copolymers.

Polymer	Source						Product	
	PEG-P(Asp)[a]	BzlBr		DBU		BnBr/DBU	Yield	D.s. Bzl[b]
	g (Asp mmol)	g (mmol)	mol.eq./Asp	g (mmol)	mol.eq./Asp		(mg)	(%)
3	0.501 (1.51)	0.261 (1.52)	1.01	0.200 (1.31)	0.87	1.16	0.597	80
4	0.501 (1.51)	0.172 (1.00)	0.66	0.141 (0.93)	0.61	1.08	0.531	53
5	0.501 (1.51)	0.115 (0.67)	0.44	0.093 (0.61)	0.40	1.10	0.516	33

[a] PEG-P(Asp) 5-24 was prepared by hydrolysis of PEG-PBLA 2.
[b] Degree of benzyl substitution.

Please cite this article as: T. Satoh, et al., Encapsulation of the synthetic retinoids Am80 and LE540 into polymeric micelles and the retinoids' release control, J. Control. Release (2009), doi:10.1016/j.jconrel.2009.02.024

2.2.2. Synthesis of PEG-b-poly(aspartic acid) (PEG-P(Asp))

Benzyl ester of PEG-PBLA **2** was hydrolyzed in 0.5 M aqueous sodium hydroxide solution (3 mol.eq. to benzyl group) at r.t. In approximately 20 min, a suspension of the polymer changed into a transparent solution owing to hydrolysis. The resulting solution was acidified with 6 M hydrochloric acid, dialyzed against water, and freeze-dried. Chemical structures of products were analyzed by ^{1}H-NMR spectroscopy in deuterium oxide containing sodium deuteroxide. The peaks assigned to the benzyl group completely disappeared on the spectrum, indicating hydrolysis of the benzyl ester. The DP of the poly(aspartic acid) chain decreased from 28 to 24 in this step. It was also confirmed that the α-amide bond in the PBLA main chain was converted into the mixture of α- and β-amides (ca. 1:3) as described in previous reports [26,28].

2.2.3. Synthesis of partially benzyl-substituted PEG-P(Asp) (PEG-P(Asp (Bzl)x))

Partially benzyl-substituted PEG-P(Asp) (PEG-P(Asp $(Bzl)_x$)) polymers **3**–**5** were obtained by esterification of PEG-P(Asp) with benzyl bromide in the presence of 1,8-diazabicyclo[5.4.0]undec-7-ene (DBU) as reported in a previous paper [29]. The number *x* in the PEG-P(Asp $(Bzl)_x$) formula represents a percentage (%) of benzyl ester in the aspartic acid residues. PEG-P(Asp) was dissolved to DMF and was added by means of BzlBr and DBU, and the reaction mixture was stirred at 50 °C for 16 h under a nitrogen atmosphere. Polymers **3**, **4**, and **5** were obtained when BzlBr was added in 1.01, 0.66, and 0.44 mol. eq. to the aspartic acid unit, respectively, while the BzlBr/DBU mole ratio was almost constant ca. 1.1. The reaction mixture was dropwisely added into diethyl ether. The resulting precipitate was collected by filtration, washed with diethyl ether, and dried under a reduced pressure. For removal of DBU, the polymers were dissolved into DMF, followed by the addition of 6 M hydrochloric acid (1 mol.eq. to DBU), and then this mixture solution was dialyzed against water. The purified products were freeze-dried and analyzed by ^{1}H-NMR spectroscopy in DMSO-d_6 containing 3% trifluoroacetic acid. Table 1 summarizes the degree of benzyl substitution determined from a proton integration ratio between methylene of PEG (3.7–3.4 ppm) and methylene of the benzyl group (5.1–5.0 ppm).

2.3. Preparation of micelles

Drug-encapsulating micelles were obtained by a solvent evaporation method [30]. The process was as follows: the block copolymer (20 mg) and the drug (2.0 mg) were dissolved in THF (2.5 mL). Evaporation of THF with stirring at 40 °C under a dry nitrogen-gas flow provided a residue of the polymer and the drug as a thin-film. The residue was further dried under a reduced pressure, and then added by water (4.0 mL). A drug-encapsulating micelle was formed by subsequent sonication with a VCX-750 sonicator equipped with a 5 mm diameter microtip (Sonic & Materials Inc., CT, USA). The sonication was operated at 21% amplitude with 80-cycle of a 0.5 s pulse followed by a 1.0 s pause, at r.t. The micelle solution was centrifuged to remove a possible insoluble precipitate (3900 rpm, 10 min, 20 °C) and then filtered through a Millex 0.22 μm PVDF filter (Nihon Millipore K.K., Tokyo, Japan). The obtained micelle solution was stored at −30 °C before use. Empty micelles were prepared according to the same procedure in the absence of drug. When an additive compound was used, the compound was mixed in the initial polymer-drug solution.

2.4. Measurements of drugs encapsulated in micelles

Drug amounts recovered in the micelle solutions were determined by reversed phase HPLC. The mobile phase involved methanol–5% acetic acid aqueous solution mixture at 2:1 (v/v) for Am80 and 9:1 (v/v) for LE540. A flow rate was 1.0 mL/min at 40 °C. Detection was carried out by absorption at 290 nm and 356 nm for Am80 and LE540, respectively.

2.5. In vitro drug release

The drug-encapsulating micelle solution (1.0 mL) was filled in a dialysis tube and dialyzed against 100-fold volume of water or Dulbecco's phosphate buffer saline (D-PBS, pH 7.4) with stirring at r.t. An aliquot of the dialysate was freeze-dried prior to the addition of methanol (100 μL). After centrifugation (10,000 g, 10 min, r.t.), the resulting supernatant was applied to the reverse-phased HPLC system for measurements of the released drugs. This drug-release assay was performed in triplicate except as described elsewhere. The error bars represent the standard deviation.

2.6. Measurements of N,N-dimethyldodecylamine (DMDA) encapsulated in micelles

The micelles of polymer **1** (20 mg) were prepared through the evaporation–sonication process in the presence of Am80 (2.0 mg, 5.69 μmol) and *N*,*N*-dimethyldodecylamine (DMDA, 1.2 mg, 5.69 μmol) in water (4.0 mL). After the centrifugation and filtration, the resulting solution (500 μL) was ultrafiltered (10,000 g, 25 min, r.t.) with a Microcon YM-100 centrifugal filter unit (Nihon Millipore K.K., Tokyo, Japan). Fresh water (200 μL) was added to a retentate and ultrafiltered again (10,000 g, 20 min, r.t.). This water-addition–ultrafiltration cycle was repeated three times. The retentate and the filtrate were collected and their contents of Am80 and DMDA were determined by means of a reversed-phase HPLC. Measurement conditions for DMDA were as follows: the mobile phase was methanol–water at 9:1 (v/v) containing 0.1% (v/v) of triethylamine, the flow rate was 1.0 mL/min at 40 °C, and detection of DMDA was carried out with an RI detector. This experiment was performed in triplicate. The other sample solutions containing different compositions were prepared for the comparison as shown in Table 5.

2.7. Statistics

Each release study was performed in triplicate except for specifically indicated cases. Data were expressed as the mean ± standard deviation (SD). Statistical comparisons were performed by the use of two-tailed Student's *t*-test for two-groups, and Dunnett's method by the use of a JMP Version 6 Japanese edition software (SAS Institute Japan, Tokyo) for multiple groups.

3. Results and discussion

3.1. Preparation of drug-encapsulating micelles

PEG-PBLA polymers **1** and **2** were successfully prepared according to literatures (see experimental section). Polymer **2** was converted into PEG-P(Asp $(Bzl)_x$) **3**–**5** through hydrolysis of **2** and subsequent benzyl-esterification (Scheme 1). The degree of benzyl substitution of **3**–**5** was controlled with feed amounts of BzlBr and DBU (Table 1). The micelles from polymers **1** and **3**–**5** were obtained by means of a solvent evaporation–sonication technique. The evaporation process resulted in formation of a thin film composed of a mixture of polymer and drug. Subsequent sonication of this film in water provided a drug-encapsulating polymeric micelle solution.

It is worth pointing out that both Am80 and LE540 were very efficiently encapsulated in the PEG-PBLA and PEG-P(Asp $(Bzl)_x$) polymer micelles (Table 2). A high encapsulation yield of ≥75% of the feed was demonstrated on all polymers examined in the wide range of 33 to 100% of the degree of benzyl substitution. Any precipitate was not formed, and furthermore, insoluble aggregates did not interfere with the filtration. When PEG-P(Asp $(Bzl)_x$) polymers

Please cite this article as: T. Satoh, et al., Encapsulation of the synthetic retinoids Am80 and LE540 into polymeric micelles and the retinoids' release control, J. Control. Release (2009), doi:10.1016/j.jconrel.2009.02.024

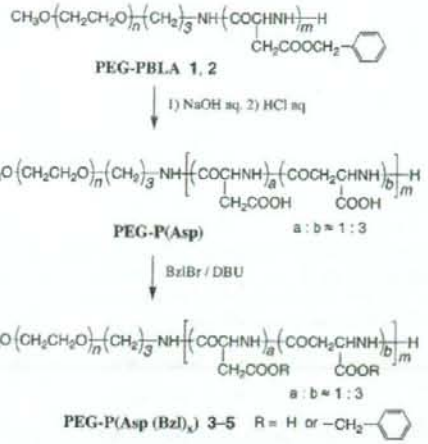

Polymer	n	m	D.s. Bzl* (%)
1	117	24	100
2	117	28	100
3	117	24	80
4	117	24	53
5	117	24	33

* Degree of benzyl substitution.

Scheme 1. Synthetic scheme of PEG-P(Asp (Bzl)$_x$) from PEG-PBLA.

encapsulated a hydrophobic drug, camptothecin, the benzyl substitution degree significantly affected the drug encapsulation efficiency [29]. It was reported that an encapsulation yield of camptothecin reached >90% at 69% of the benzyl substitution degree, however, the yield decreased to <40% at 44% of the substitution. In contrast, Am80 and LE540 were encapsulated at high yields in a wide range of the benzyl ester content of PEG-P(Asp (Bzl)$_x$).

Transparent solutions from polymers **3** and **4** and very faintly hazy ones from polymers **1** and **5** were obtained by means of the evaporation–sonication technique in the presence of a drug. It is important to note that Am80 and LE540 themselves were almost insoluble in water. When the evaporation–sonication technique was applied to the drugs without a polymer, only a slight amount of the drugs (<1% of the feed) was detected in supernatants after the centrifugation. The remaining part of the feed drugs was separated as precipitates. These results indicated that the faintly hazy appearance of the micelle solutions from polymers **1** and **5** was due to particle sizes ≥ca. 140 nm of the polymeric micelles (Table 2), not due to dispersed free drug aggregates.

Interestingly, very low intensity of scattered light was observed in a DLS measurement for a solution of polymer **5** through the evaporation–sonication process without a drug. This result indicated that polymer **5** alone did not form micelle structures as clearly as polymers **1**, **3**, and **4** owing to its low degree (33%) of hydrophobic benzyl substitution. This block copolymer **5** obtained sufficient hydrophobicity to distinctly form micellar structures by physically entrapping the hydrophobic drug. This preferential contribution of the encapsulated drug to the micelle formation can expand choices of block copolymer compositions. Block copolymers possessing hydrophobicity insufficient for the micelle formation can be used for micelle drug-carrier systems if these polymers are successfully given additional hydrophobicity by the encapsulated drugs. This was reported for chemical conjugation of drugs to block copolymers [31], in a doxorubicin-conjugated PEG-P(Asp) system. In contrast, for this Am80 case, the drug was encapsulated in a much easier way, physical entrapment. As far as we know, this is the first report regarding this type of preferential contribution of the physically entrapped drug to polymeric micelles' formation.

Table 2
Encapsulation yield of the drugs and particle size distributions of the polymeric micelles.[a]

Polymer	Am80 encapsulation		LE540 encapulation		Empty
	% Drug encapsulated	Particle size (nm); weight fraction	% Drug encapsulated	Particle size (nm); weight fraction	Particle size (nm); weight fraction
1	94	42±9; 81% 151±29; 19%	82	52±10; 71% 148±28; 29%	60±28; 100%
3	105	21±4; 100%	109	17±3;92% 73±13;8%	7±1; 85% 21±4; 15%
4	101	20±4; 100%	100	23±5; 100%	17±3;100%
5	75	188±37;94% 817±91;6%	94	54±8; 66% 137±24; 34%	–[b]

[a] Weight distributions.
[b] Very low intensity of scattered light.

3.2. Drug release from micelles in vitro

In vitro drug-release rates were measured by means of a dialysis method. The sealed dialysis bag containing the drug-encapsulating micelle solution was placed in a container of D-PBS or water. Using HPLC, we monitored the drug's release from the micelles into an aqueous medium outside the dialysis bag. The experiments were carried out by the use of the micelle solutions summarized in Table 2. These micelle solutions contained Am80 and LE540 in the concentration range of 0.37–0.53 mg/mL and 0.41–0.54 mg/mL, respectively.

A rapid release of Am80 occurred in D-PBS. Approximately 60% of the encapsulated Am80 was released within 8 h for all polymers as shown in Fig. 1. We observed no influence of the polymers' benzyl substitution degree on the release rate. Am80 was soluble in D-PBS at ≥200 μg/mL at r.t. as opposed to Am80's poor solubility of 2 μg/mL in water under the same conditions. Such high solubility in D-PBS is likely to accelerate the rapid release. The observed release rates in this evaluation seem to be too fast for drug targeting purposes, since a blood-circulation period of 24 h or more was necessary for the EPR effect's efficient passive targeting to a solid tumor tissue [2]. The rapid drug-release behaviors shown in Fig. 1 suggest a situation where most of the encapsulated drug is released in the blood stream before the drug carrier system accumulates at the tumor tissue.

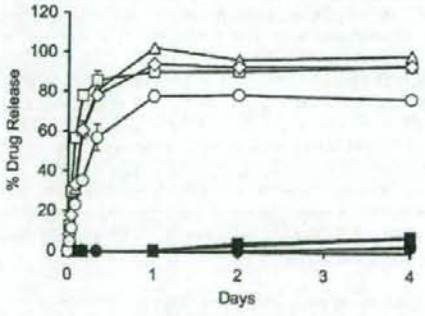

Fig. 1. Release of Am80 and LE540 from the polymeric micelles at r.t. in D-PBS (mean ± SD, $n = 3$). The drug-encapsulating micelles were prepared from polymer **1** (circle), **3** (diamond), **4** (triangle), and **5** (square). Open and filled symbols indicate Am80 and LE540, respectively. The amounts of drug encapsulated in polymeric micelles were normalized to 100%.

Please cite this article as: T. Satoh, et al., Encapsulation of the synthetic retinoids Am80 and LE540 into polymeric micelles and the retinoids' release control, J. Control. Release (2009), doi:10.1016/j.jconrel.2009.02.024

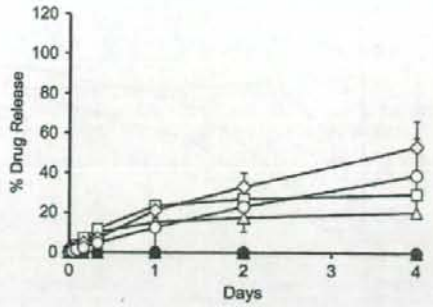

Fig. 2. Release of Am80 and LE540 from the polymer micelles at r.t. in water (mean ± SD, $n = 3$). The drug-encapsulating micelles were prepared from polymer **1** (circle), **3** (diamond), **4** (triangle), and **5** (square). Open and filled symbols indicate Am80 and LE540, respectively. The amounts of drug encapsulated in polymeric micelles were normalized to 100%.

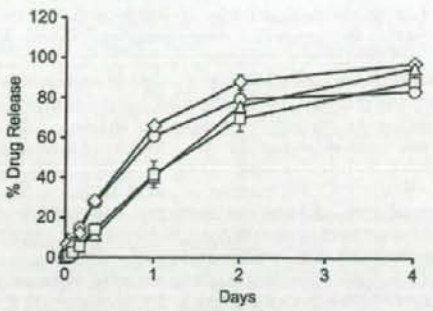

Fig. 3. Release of Am80 from the polymeric micelles at r.t. in D-PBS (mean ± SD, $n = 3$). The Am80-encapsulating micelles were prepared from polymer **1** (circle), **3** (diamond), **4** (triangle), and **5** (square) in the presence of DMDA at various molar ratios to Am80 (circle = 1, diamond = 2.7, triangle = 5.4, and square = 7.5). The amounts of drug encapsulated in polymeric micelles were normalized to 100%.

As compared with the release in D-PBS, considerable release retardation of Am80 was observed in water as shown in Fig. 2. Accumulated Am80 release amounts after 8 h were only 5–12%. Even 4 days later, the released Am80 amounts remained in a range of 20–53%. These results demonstrated that the release rates of Am80 in D-PBS as a dialysate were dramatically differed from the release rates to Am80 in water as a dialysate. This difference was probably due to a difference in Am80 solubility in these solvents. In the release experiments in water, small amounts of powdery precipitates appeared in the dialysis bag within 1–2 days except for the micelles of polymer **1**. This precipitate seems to have been the released Am80. The poor solubility of Am80 in water is likely to lead to saturation in the dialysis bag prior to Am80's diffusion into the exterior. All these results imply that the poor Am80 solubility in water favors very high encapsulation efficiency, and that the higher solubility in D-PBS than in water causes a rapid release of Am80 from micelles.

In contrast, LE540 was scarcely released either in D-PBS or in water throughout the time period examined, indicating LE540's very stable encapsulation of the synthetic retinoid into the polymeric micelles, as shown in Figs. 1 and 2. Only 3–8% of release was observed in D-PBS over the course of 4 days. This stable encapsulation probably resulted from stronger hydrophobicity of LE540 than of Am80.

3.3. Addition of *N,N*-dimethyldodecylamine (DMDA)

To accomplish more stable encapsulation of Am80, we investigated complex formation of Am80 with a hydrophobic additive. A hydrophobic fatty amine was selected for this purpose. First, *N,N*-dimethyldodecylamine (DMDA) was mixed with Am80 and the polymer in THF, and the mixture was applied to the evaporation–sonication process for the encapsulation. The molar ratio of DMDA to Am80 (DMDA/Am80) was adjusted to 1.0, 2.7, 5.4, and 7.5 for the micelles of polymers **1**, **3**, **4**, and **5**, respectively. These amounts of DMDA corresponded to the molar equivalent of all carboxyl groups of Am80 and aspartic acid residue of a polymer. High Am80 encapsulation yields >94% were confirmed (Table 3; Entries 1, 5, 7, and 9), indicating that the presence of DMDA did not lower the drug encapsulation efficiency. The particle sizes of the polymeric micelles prepared with DMDA did not show a substantial change compared with those prepared without this additive (Table 3; Entries 1, 5, and 7). The only exception was the case of polymer **5**, where the particle diameter decreased from ca. 200 nm to <10 nm upon the addition of DMDA (Table 3; Entry 9). This unique result was found only for polymer **5**, which exhibited distinctive micelle formation only after encapsulation of Am80. (As described above, only polymer **5** did not form a micelle structure.) Although the mechanism for this behavior has not been elucidated, this exceptional result was not observed for the other polymers that formed micelle structures even in the absence of the encapsulated drug.

A remarkable effect of the DMDA addition was a significant retardation in Am80 release from the polymeric micelles in D-PBS, as shown in Fig. 3. A period of 2 days was necessary to attain 60% release of the encapsulated Am80, while the same amounts were rapidly released within 8 h in the absence of DMDA (Fig. 1). At 8 h of the release period, the retardation of Am80 release by means of the DMDA addition indicated statistically significant differences ($P<0.05$) in each polymeric micelle as compared with each micelle without the DMDA addition.

Two mechanisms should be considered to explain these results. The first is a hydrophobic complex formation of Am80 between DMDA. A hydrophilic carboxylic group of Am80 is assumed to greatly

Table 3
Encapsulation of Am80 into the polymeric micelles in the presence of DMDA.

Entry	Polymer	DMDA/Am80[a]	% AM80 encapsulated	Particle size (nm); weight fraction
1	**1**	1	94	36±4; 56%, 135±26; 24%, 639±110; 20%
2	**1**	2.7	97	43±8; 77%, 135±25; 17%
3	**1**	5.4	103	66±24; 89%, 679±109; 11%
4	**1**	7.5	101	54±14; 77%, 817±102; 23%
5	**3**	2.7	97	14±0; 64%, 32±7; 35%, 817±102; 1%
6	**4**	1	100	24±7; 100%
7	**4**	5.4	101	13±2; 97%, 39±8; 3%
8	**4**	10.7	90	22±4; 100%
9	**9**	7.5	104	4±0; 74%, 8±1; 26%

N,N-dimethyldodecylamine (DMDA)

[a] Molar ratio.

Please cite this article as: T. Satoh, et al., Encapsulation of the synthetic retinoids Am80 and LE540 into polymeric micelles and the retinoids' release control, J. Control. Release (2009), doi:10.1016/j.jconrel.2009.02.024

contribute to the high solubility of Am80 in D-PBS. Therefore, conversion of this group to a more hydrophobic state is probably effective in decreasing the solubility. An ionic compound's solubility can be changed by means of an electrostatic interaction between an opposite charged hydrophobic compound, and researchers have used the effect as the "hydrophobic ion-pairing" technique [32,33]. This technique serves to increase the hydrophobicity of hydrophilic ionic compounds including a drug [33,34] as well as a protein and polynucleotide [32]. For example, a potent antituberculosis drug, isonicotinic acid hydrazide, was chemically converted into an ionic compound as a prodrug, and the hydrophobic ion-pairing significantly enhanced drug's solubility to an organic solvent [33]. Furthermore, skin accumulation of retinoic acid was enhanced by an ion-pairing with a series of hydrophobic amino acid methyl esters [34]. In our study, DMDA is regarded as a hydrophobic counter partner for Am80. This is the first report that the ion-pairing technique has been used for stable drug encapsulation in the polymeric micelle carrier system.

The second mechanism that explains the effect of DMDA is a change of micellar core characteristics by encapsulation of a hydrophobic additive. Forrest et al. reported that encapsulation of α-tocopherol (vitamin E) into PEG-*b*-poly(ε-caprolactone) (PEG-PCL) micelles decreased the viscosity of the crystalline PCL core owing to dispersed microphases of α-tocopherol [23]. Such a plasticized PCL core was receptive to a larger amount of rapamycin loading. Furthermore, the α-tocopherol-co-encapsulating micelle demonstrated a retardation of the drug release in PBS containing bovine serum albumin as compared with the PEG-PCL micelle formed without α-tocopherol.

If DMDA contributes to the sustained release of Am80 mainly by means of the hydrophobic ion-pairing, this contribution increases up to the DMDA addition at the DMDA/Am80 molar ratio of 1. On the other hand, if DMDA acts to change the characteristics of the micellar core, the retardation effect by DMDA relies on the amount of added DMDA beyond the DMDA/Am80 ratio of 1. Therefore, we investigated the effects of an added DMDA amount by using polymers **1** and **4**. When DMDA was added to a mixture of polymer **1** and Am80 in the range of the DMDA/Am80 ratio from 1.0 to 7.5 (Table 3; Entries 1–4), the drug-release rate underwent no significant changes, as shown in Fig. 4. This result indicated that the retardation of the Am80 release was due to the hydrophobic ion-pairing of Am80 and DMDA for the polymer **1** case. On the other hand, the retardation of the drug release was observed at the DMDA/Am80 ratio ≥ 5.4 for the micelle of polymer **4** as shown in Fig. 5. The retardation effect hardly exhibited itself at the DMDA/Am80 ratio of 1. This deficient retardation was probably due to the presence of the carboxyl group of polymer **4**. This carboxyl group would compete with the carboxyl group of Am80 for interaction with DMDA. Therefore the excess amount of DMDA going to Am80 was necessary for the obvious retardation. In fact, the molar amount of DMDA at a DMDA/Am80 molar ratio of 5.4 in which the substantial retardation effect was demonstrated was equal to the molar amount of all the carboxyl groups of Am80 and polymer **4**. Two mechanisms serve to explain the observed retardation, as shown in Fig. 5. The first is an increase in the hydrophobicity of Am80 caused by the ion-pairing with DMDA as described above. The second is a change of characteristics of the micelle inner core accompanying the pairing of the carboxyl group of polymer **4** and DMDA. It is difficult to indicate which mechanism dominantly contributed to the retardation, since the current study did not separate the effect on Am80 from that on the polymer.

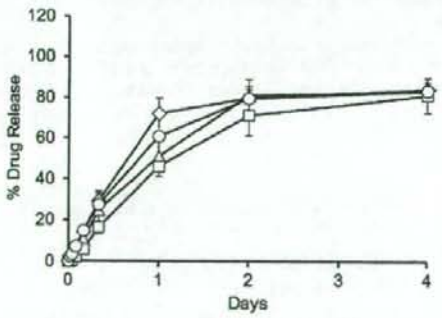

Fig. 4. Release of Am80 from the micelles of polymer **1** at r.t. in D-PBS (mean ± SD, $n = 3$). The Am80-encapsulating micelles were prepared in the presence of DMDA at various molar ratios to Am80 (circle = 1, diamond = 2.7, triangle = 5.4, and square = 7.5). The result at the ratio of 1 represented in Fig. 3 was shown again for the comparison with the results at the other ratios. The amounts of drug encapsulated in polymeric micelles were normalized to 100%.

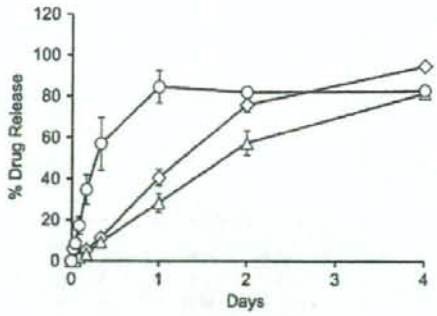

Fig. 5. Release of Am80 from the micelles of polymer **4** at r.t. in D-PBS (mean ± SD, $n = 3$). The Am80-encapsulating micelles were prepared in the presence of DMDA at various molar ratios to Am80 (circle = 1, diamond = 5.4, and triangle = 10.7). The result at the ratio of 5.4 represented in Fig. 3 was shown again for the comparison with the results at the other ratios. The amounts of drug encapsulated in polymeric micelles were normalized to 100%.

Zeta potential of empty polymeric micelles except for the micelles of polymer **5** was −5.6 ± 0.2 to −12.6 ± 1.3 mV; see Supplementary Table S1. These values were slightly decreased with the Am80 encapsulation (−9.9 ± 0.0 to −22.1 ± 0.7 mV). Although the DMDA addition raised the zeta potential, the micelles kept negative surface charges under the conditions for the retardation experiments of the Am80 release.

As described above, the addition of DMDA successfully triggered the retardation of the Am80 release. The presumption is that the triggering mechanism involved the hydrophobic complex formation between Am80 and DMDA, and the encapsulation of this complex in the polymeric micelle. Therefore, we investigated not only Am80 but also the co-encapsulation of DMDA into the polymeric micelle.

The polymeric micelle solutions prepared in the presence of Am80 and DMDA were ultrafiltered with a Microcon YM-100 (100-kDa cut-off). This process separated the polymeric micelles in the retentate from low-molecular compositions in the filtrate. A retentate is a residual solution on an ultrafilter membrane after the ultrafiltration, and a filtrate is a solution that has passed through the ultrafilter. The amounts of Am80 and DMDA both in the retentate and the filtrate were measured by means of an HPLC. Six samples were applied to this separation experiment, as summarized in Table 4. The sample solutions included DMDA, polymer **1**, and Am80 (Entry 1), DMDA alone (Entries 2 and 3), DMDA and polymer **1** (Entry 4), and DMDA and Am80 (Entries 5 and 6). We prepared the solutions by using the evaporation–sonication process.

Approximately 76% of the feed DMDA was recovered in the sample solutions prepared in the presence of polymer **1** and Am80 (Table 4;

Please cite this article as: T. Satoh, et al., Encapsulation of the synthetic retinoids Am80 and LE540 into polymeric micelles and the retinoids' release control, J. Control. Release (2009), doi:10.1016/j.jconrel.2009.02.024

Table 4
Compositions of sample solutions for the separation experiments and percent recovery of DMDA and Am80.

Entry	Feed				% Recovered					
	DMDA mg (μmol)	Polymer 1 mg	Am80 mg (μmol)	DMDA/Am80[a]	DMDA			Am80		
					Sample solution	Retentate[b]	Filtrate[b]	Sample solution	Retentate*	Filtrate **
1	1.2 (5.69)	20.0	2.0 (5.69)	1	75.8	50.7 ± 1.5	9.7 ± 1.2	83.9	63.2 ± 0.4	0.2 ± 0.0
2	1.2 (5.69)	–	–	–	0	–	–	–	–	–
3	6.5 (30.5)	–	–	–	10.7	0	8.7 ± 0.5	–	–	–
4	1.2 (5.69)	20.0	–	–	28.6	4.5 ± 0.4	13.3 ± 1.7	–	–	–
5	1.2 (5.69)	–	2.0 (5.69)	1	0	–	–	0.4	–	–
6	6.5 (30.5)	–	2.0 (5.69)	5.4	17.7	N.D.[c]	13.5 ± 0.5	100.1	N.D.***	35 ± 0.7

[a] Molar ratio.
[b] Mean ± SD ($n = 3$).
[c] N.D. means not determined.

Entry 1). This recovered DMDA remained in the retentate (50.7% of the feed) even after the ultrafiltration (Table 4; Entry 1). Simultaneously, we observed that Am80 in this sample solution was 83.9% of the feed. Moreover, after the ultrafiltration, 63.2% of the feed remained in the retentate, and only 0.2% of the feed was found in the filtrate. In contrast, in the examination for DMDA alone, we observed that a serious loss of feed DMDA (only recovered < 11% of the feed) probably caused by adsorption of DMDA to a 0.22 μm filter in the sample preparation process (Table 4; Entries 2 and 3). Moreover, almost all of the recovered DMDA was ultrafiltered into the filtrate, and no DMDA was found in the retentate (Table 4; Entry 3). Remaining DMDA (ca. 20%) was probably adsorbed to a Microcon YM-100 filter. These results support the assertion that both Am80 and DMDA were encapsulated into polymeric micelles. Although the encapsulation of DMDA into polymeric micelles was also observed in the absence of Am80 (Table 4; Entry 4), DMDA in the sample solution was only <30% of the feed (Table 4; Run 4). In addition, a half of the recovered DMDA was ultrafiltered into the filtrate. Therefore, the stable encapsulation of DMDA in the micelles of polymer **1** was achieved by means of the co-encapsulation of DMDA with Am80.

When DMDA was mixed with Am80 at an equal molar ratio (DMDA/Am80 = 1), an insoluble aggregate was formed during sonication. After removal of the aggregate by means of centrifugation, no DMDA and only 2 μg/mL of Am80 (<1% of the feed) remained in the supernatant (Table 4; Entry 5). Under the same conditions in the presence of polymer **1**, such an insoluble aggregate was not observed, and a high encapsulation yield of Am80 (84%) was obtained (Table 4; Entry 1). These contrast results indicate two points: first, the complex of Am80 and DMDA that formed at DMDA/Am80 of 1 was insoluble in water, and second, the solubilization of the complex depended on encapsulation of the complex into the polymeric micelles. In contrast to the results at DMDA/Am80 = 1, the mixture at DMDA/Am80 = 5.4 provided a transparent solution by means of sonication. This solution contained 17.7% and 100% of the feed for DMDA and Am80, respectively, indicating that DMDA both formed a low-molecular micelle and encapsulated Am80 (Table 4; Entry 6). This Am80-DMDA solution, however, formed an insoluble aggregate in the retentate during the ultrafiltration procedure. Almost all of the recovered DMDA was ultrafiltered into the filtrate. In contrast, only 3.5% of the feed Am80 was found in the filtrate. This result implied that the Am80-encapsulating DMDA micelles were dissociated in the ultrafiltration and that the Am80 was no longer encapsulated in the DMDA micelles. In addition, this result also indicated that the retardation of the Am80 release was not caused by a sustained release from the Am80-encapsulating DMDA micelle. If Am80 had been dominantly encapsulated in the DMDA micelle but not the polymeric micelle, the aggregate would have been observed in the ultrafiltration of the experiment for Entry 1. In fact, no such aggregate was observed. Therefore, the retarded release of Am80 was accomplished by the co-encapsulation of the drug and DMDA in the polymeric micelles.

3.4. Effects of an additive's structure on the release of Am80

We investigated the effects that chemical structure of an additive has on the retardation of Am80 release by using six kinds of amines, as shown in Chart 2. We added these amines to the encapsulation process of the Am80. The added amounts of the additives were adjusted to additive/Am80 molar ratio of 1. The micelles were prepared from polymer **1** in order to ignore the influence of the carboxyl groups of the polymer. High Am80 encapsulation yields between of 61% and 96% were obtained in all additives examined as summarized in Table 5.

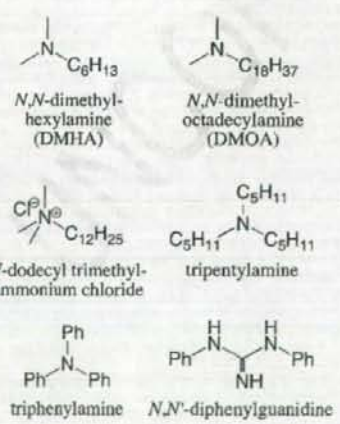

Chart 2. Amines examined for the retardation effect on the Am80 release.

Table 5
Encapsulation of Am80 into the polymeric micelles in the presence of various additives.

Entry	Additive	% Am80 encapsulated	Particle size (nm); weight fraction
1	*N,N*-dimethylhexylamine	96	86 ± 14; 79%, 215 ± 36; 21%
2	*N,N*-dimethyloctadecylamine	80	74 ± 13; 22%, 231 ± 45; 78%
3	*N*-dodecyltrimethylammonium chloride	78	69 ± 13; 71%, 195 ± 37; 29%
4	Tripentylamine	61	65 ± 11; 86%, 185 ± 33; 14%
5	Triphenylamine	88	79 ± 14; 76%, 224 ± 41; 24%
6	*N,N'*-diphenylguanidine	91	34 ± 6; 87%, 138 ± 24; 13%

Please cite this article as: T. Satoh, et al., Encapsulation of the synthetic retinoids Am80 and LE540 into polymeric micelles and the retinoids' release control, J. Control. Release (2009), doi:10.1016/j.jconrel.2009.02.024

The Am80 release was measured once for each additive-co-encapsulating micelle, as shown in Fig. 6. Of the six additives, *N,N*-dimethyloctadecylamine (DMOA) demonstrated the largest retardation effect on the Am80 release. The other five additives showed only small effects for the retardation. These results were likely caused either by undesired steric hindrance, inhibiting the interaction between Am80 and the amines, or by an insufficient increase in the hydrophobicity of the Am80-complex. A series of the *N,N*-dimethylalkylamines exhibit a decrease the release rates of Am80 with an increase of the alkyl chain length. This effect was confirmed in separate triplicate examinations as shown in Fig. 7. A comparison of three *N,N*-dimethylalkylamines, i.e., DMOA, DMDA, and *N,N*-dimethylhexylamine (DMHA), clearly showed the effect of the chain length. This result indicates that the counter additive selection can control the release rate of Am80 from a polymeric micelle. At 1 day of the release period, the retardation effects by means of DMOA or DMDA addition were statistically significant (DMOA; $P<0.001$ and DMDA; $P<0.01$) in comparison with the control group (encapsulation of Am80 alone; filled square in Fig. 7). On the other hand, a difference from the control system by means of DMHA addition was statistically insignificant at $P>0.05$.

Cytotoxicities of *N,N*-dimethylalkylamines were evaluated by means of a standard in vitro cytotoxicity test; see Supplementary Fig. S1. The results were compared with that of 1-octadecylamine (stearylamine), frequently used in vivo as a component of liposomal carriers [35]. DMDA and DMOA, two additives that showed sufficient retarded release effect, exhibited a similar cytotoxicity to 1-octadecylamine. These results indicate that toxicity of these additives can be acceptable to use in vivo depending on toxicity of encapsulated drugs. DMHA, hardly effective for retarded release, exhibited no cytotoxicity up to 100 μM. The next challenge is in vivo studies to validate this release rate control by means of the ion-pairing technique.

4. Conclusions

Two synthetic retinoids, Am80 and LE540, were encapsulated into block copolymer micelles, and the encapsulation was both highly efficient and exceptionally facile. An in vitro release examination for LE540 demonstrated very stable encapsulation of this drug. As for Am80, it was rapidly released in D-PBS in contrast to Am80's sustained release in water. We triggered a retardation of the release rate of Am80 by adding DMDA into the encapsulation process. This retardation was due to an increase in the hydrophobicity of Am80, itself caused by the ion-pairing of this retinoid with hydrophobic DMDA. The retardation effect increased with increase in the alkyl chain length of additive amines, suggesting that proper choice of an additive amine leads to optimum control of drug release. This is the first report concerning the ability of ion-pairing between a drug and an additive to promote control a drug's release rate in a polymeric micelle carrier system. This ion-pairing technique requires only the mixing of an adequate additive without any chemical modification of the drug or the polymers. Thus, it appears highly promising that this simple technique is applicable to various drugs possessing an ionic group.

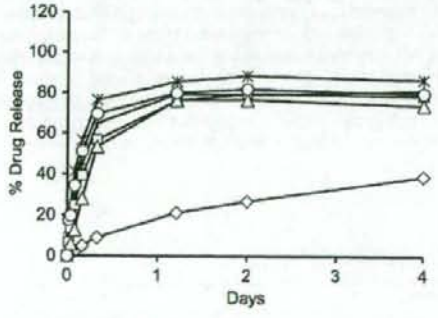

Fig. 6. Release of Am80 from the micelles of polymer **1** at r.t. in D-PBS ($n=1$). The Am80-encapsulating micelles were prepared in the presence of various amine additives at an equal molar ratio to Am80 (circle = *N,N*-dimethylhexylamine, diamond = *N,N*-dimethyloctadecylamine, triangle = *N*-dodecyltrimethylammonium chloride, square = tripentylamine, asterisk = triphenylamine, and cross = *N,N'*-diphenylguanidine). The amounts of drug encapsulated in polymeric micelles were normalized to 100%.

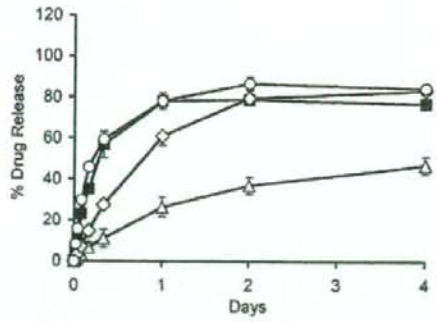

Fig. 7. Release of Am80 from the micelles of polymer **1** at r.t. in D-PBS (mean ± SD, $n=3$). The Am80-encapsulating micelles were prepared in the presence of various *N,N*-dimethylalkylamines at an equal molar ratio to Am80 (circle = *N,N*-dimethylhexylamine, diamond = *N,N*-dimethyldodecylamine, triangle = *N,N*-dimethyloctadecylamine, and filled square = no additive). The results of *N,N*-dimethyldodecylamine represented in Fig. 3 and no additive group represented in Fig. 1 were shown again for the comparison with the results of the other groups. The amounts of drug encapsulated in polymeric micelles were normalized to 100%.

Appendix A. Supplementary data

Supplementary data associated with this article can be found, in the online version, at doi:10.1016/j.jconrel.2009.02.024.

References

[1] S.R. Croy, G.S. Kwon, Polymeric micelles for drug delivery, Curr. Pharm. Des. 12 (2006) 4669–4684.
[2] Y. Matsumura, H. Maeda, A new concept for macromolecular therapeutics in cancer chemotherapy: mechanisms of tumoritropic accumulation of protein and the antitumor agent SMANCS, Cancer Res. 46 (1986) 6387–6392.
[3] M. Yokoyama, T. Okano, Y. Sakurai, S. Fukushima, K. Okamoto, K. Kataoka, Selective delivery of adriamycin to a solid tumor using a polymeric micelle carrier system, J. Drug Target. 7 (1999) 171–186.
[4] M.L. Forrest, J.A. Yáñez, C.M. Remsberg, Y. Ohgami, G.S. Kwon, N.M. Davies, Paclitaxel prodrugs with sustained release and high solubility in poly(ethylene glycol)-*b*-poly(ε-caprolactone) micelle nanocarriers: pharmacokinetic disposition, tolerability, and cytotoxicity, Pharm. Res. 25 (2008) 194–206.
[5] M. Watanabe, K. Kawano, M. Yokoyama, P. Opanasopit, T. Okano, Y. Maitani, Preparation of camptothecin-loaded polymeric micelles and evaluation of their incorporation and circulation stability, Int. J. Pharm. 308 (2006) 183–189.
[6] M. Sumitomo, F. Koizumi, T. Asano, A. Horiguchi, K. Ito, T. Asano, T. Kakizoe, M. Hayakawa, Y. Matsumura, Novel SN-38-incorporated polymeric micelle, NK012, strongly suppresses renal cancer progression, Cancer Res. 68 (2008) 1631–1635.
[7] S. Kawakami, P. Opanasopit, M. Yokoyama, N. Chansri, T. Yamamoto, T. Okano, F. Yamashita, M. Hashida, Biodistribution characteristics of all-*trans* retinoic acid incorporated in liposomes and polymeric micelles following intravenous administration, J. Pharm. Sci. 94 (2005) 2606–2615.
[8] T. Okuda, S. Kawakami, M. Yokoyama, T. Yamamoto, F. Yamashita, M. Hashida, Block copolymer design for stable encapsulation of *N*-(4-hydroxyphenyl)retinamide into polymeric micelles in mice, Int. J. Pharm. 357 (2008) 318–322.
[9] IUPAC-JUB Joint Commission on Biochemical Nomenclature (JCBN), Nomenclature of retinoids. Recommendations 1981, Pure Appl. Chem. 55 (1983) 721–726.
[10] A.L. Fields, D.R. Soprano, K.J. Soprano, Retinoids in biological control and cancer, J. Cell Biochem. 102 (2007) 886–898.
[11] E. Garattini, M. Gianni, M. Terao, Retinoids as differentiating agents in oncology: a network of interactions with intracellular pathways as the basis for rational therapeutic combinations, Curr. Pharm. Des. 13 (2007) 1375–1400.
[12] Z.Y. Wang, Z. Chen, Acute promyelocytic leukemia: from highly fatal to highly curable, Blood 111 (2008) 2505–2515.

Please cite this article as: T. Satoh, et al., Encapsulation of the synthetic retinoids Am80 and LE540 into polymeric micelles and the retinoids' release control, J. Control. Release (2009), doi:10.1016/j.jconrel.2009.02.024

[13] M.B. Sporn, A.B. Roberts, D.S. Goodman (Eds.), The Retinoids, 2nd ed., Raven Press, New York, 1994.
[14] B. Davidovici, Y. Tüzün, R. Wolf, Retinoid receptors, Dermatol. Clin. 25 (2007) 525–530.
[15] E. Garattini, M. Gianni, M. Terao, Retinoid related molecules an emerging class of apoptotic agents with promising therapeutic potential in oncology: pharmacological activity and mechanisms of action, Curr. Pharm. Des. 10 (2004) 433–448.
[16] N. Hail, H. Kim, R. Lotan, Mechanisms of fenretinide-jnduced apoptosis, Apoptosis 11 (2006) 1677–1694.
[17] H. Kagechika, Novel synthetic retinoids and separation of the pleiotropic retinoidal activities, Curr. Med. Chem. 9 (2002) 591–608.
[18] H. Kagechika, K. Shudo, Synthetic retinoids: recent developments concerning structure and clinical utility, J. Med. Chem. 48 (2005) 5875–5883.
[19] T. Tobita, A. Takeshita, K. Kitamura, K. Ohnishi, M. Yanagi, A. Hiraoka, T. Karasuno, M. Takeuchi, S. Miyawaki, R. Ueda, T. Naoe, R. Ohno, Treatment with a new synthetic retinoid, Am80, of acute promyelocytic leukemia relapsed from complete remission induced by all-trans retinoic acid, Blood 89 (1997) 967–973.
[20] T. Sanda, T. Kuwano, S. Nakao, S. Iida, T. Ishida, H. Komatsu, K. Shudo, M. Kuwano, M. Ono, R. Ueda, Antimyeloma effects of a novel synthetic retinoid Am80 (Tamibarotene) through inhibition of angiogenesis, Leukemia 19 (2005) 901–909.
[21] N. Takeda, I. Manabe, T. Shindo, H. Iwata, S. Iimuro, H. Kagechika, K. Shudo, R. Nagai, Synthetic retinoid Am80 reduces scavenger receptor expression and atherosclerosis in mice by inhibiting IL-6, Arterioscler. Thromb. Vasc. Biol. 26 (2006) 1177–1183.
[22] H. Umemiya, H. Fukasawa, M. Ebisawa, L. Eyrolles, E. Kawachi, G. Eisenmann, H. Gronemeyer, Y. Hashimoto, K. Shudo, H. Kagechika, Regulation of retinoidal actions by diazepinylbenzoic acids. Retinoid synergists which activate the RXR-RAR heterodimers, J. Med. Chem. 40 (1997) 4222–4234.
[23] M.L. Forrest, C.Y. Won, A.W. Malick, G.S. Kwon, In vitro release of the mTOR inhibitor rapamycin from poly(ethylene glycol)-b-poly(ε-caprolactone) micelles, J. Control. Release 110 (2006) 370–377.
[24] W.H. Daly, D. Poche, The preparation of *N*-carboxyanhydrides of α-amino acids using bis(trichloromethyl) carbonate, Tetrahedron Lett. 29 (1988) 5859–5862.
[25] M. Yokoyama, G.S. Kwon, M. Naito, T. Okano, Y. Sakurai, K. Kataoka, Preparation of micelle-forming polymer-drug conjugates, Bioconjug. Chem. 3 (1992) 295–301.
[26] T. Yamamoto, M. Yokoyama, P. Opanasopit, A. Hayama, K. Kawano, Y. Maitani, What are determining factors for stable drug incorporation into polymeric micelle carriers? Consideration on physical and chemical characters of the micelle inner core, J. Control. Release 123 (2007) 11–18.
[27] M. Yokoyama, P. Opanasopit, T. Okano, K. Kawano, Y. Maitani, Polymer design and incorporation methods for polymeric micelle carrier system containing water-insoluble anti-cancer agent camptothecin, J. Drug Target. 12 (2004) 373–384.
[28] V. Saudek, H. Pivcová, J. Drobník, NMR study of poly(aspartic acid). II. α-, and β-peptide bonds in poly(aspartic acid) prepared by common methods, Biopolymers 20 (1981) 1615–1623.
[29] P. Opanasopit, M. Yokoyama, M. Watanabe, K. Kawano, Y. Maitani, T. Okano, Block copolymer design for camptothecin incorporation into polymeric micelles for passive tumor targeting, Pharm. Res. 21 (2004) 2001–2008.
[30] A. Lavasanifar, J. Samuel, G.S. Kwon, Micelles self-assembled from poly(ethylene oxide)-block-poly(*N*-hexyl stearate L-aspartamide) by a solvent evaporation method: effect on the solubilization and haemolytic activity of amphotericin B, J. Control. Release 77 (2001) 155–160.
[31] M. Yokoyama, S. Fukushima, R. Uehara, K. Okamoto, K. Kataoka, Y. Sakurai, T. Okano, Characterization of physical entrapment and chemical conjugation of adriamycin in polymeric micelles and their design for in vivo delivery to a solid tumor, J. Control. Release 50 (1998) 79–92.
[32] J.D. Meyer, M.C. Manning, Hydrophobic ion pairing: altering the solubility properties of biomolecules, Pharm. Res. 15 (1998) 188–193.
[33] H. Zhou, C. Lengsfeld, D.J. Claffey, J.A. Ruth, B. Hybertson, T.W. Randolph, K.Y. Ng, M.C. Manning, Hydrophobic ion pairing of isoniazid using a prodrug approach, J. Pharm. Sci. 91 (2002) 1502–1511.
[34] M. Trotta, E. Ugazio, E. Peira, C. Pulitano, Influence of ion pairing on topical delivery of retinoic acid from microemulsions, J. Control. Release 86 (2003) 315–321.
[35] E. Kajiwara, K. Kawano, Y. Hattori, M. Fukushima, K. Hayashi, Y. Maitania, Long-circulating liposome-encapsulated ganciclovir enhances the efficacy of HSV-TK suicide gene therapy, J. Control. Release 120 (2007) 104–110.

Please cite this article as: T. Satoh, et al., Encapsulation of the synthetic retinoids Am80 and LE540 into polymeric micelles and the retinoids' release control, J. Control. Release (2009), doi:10.1016/j.jconrel.2009.02.024

高分子ミセルターゲティング

横山昌幸*

合成高分子が多数会合して形成する高分子ミセルが，近年薬物キャリヤーとして研究開発されている．高分子ミセルは直径が数十～100 nm の微粒子で，この粒径はまさにナノテクノロジーが扱う中心的なサイズである．よって，高分子ミセル薬物キャリヤーシステムは，ナノテクノロジーというキーワードの下に，医学と工学が融合しての研究開発の1つの代表例である．本総説では，この高分子ミセル薬物キャリヤーシステムの概要を説明し，抗癌剤ターゲティングへの応用の現状をまとめたうえで，将来の発展方向についての意見を述べる．

はじめに

薬物ターゲティングとは，「薬物治療が必要な部位に選択的に薬物を送りこみはたらかせること」であり，このために用いられるのが薬物キャリヤーである．近年，ナノテクノロジーの医療応用の観点から，ナノサイズの薬物キャリヤーへの応用が注目されている．本総説では，このナノサイズの薬物キャリヤーのなかから，世界に先駆けて日本で発明・開発されてきた高分子ミセルシステムについて，ナノテクノロジーとの関連を盛り込みながら述べてゆく．

1．高分子ミセル薬物キャリヤーとは[1)2)]

高分子ミセルは，合成高分子からなるミセルのことで，水に溶けやすい部分(ここではAとする)と溶けにくい部分(Bとする)が共存した場合に，Bの部分が会合して形成する構造である．**図1**に最も典型的なAB型ブロックコポリマーからなる高分子ミセル型薬物キャリヤーシステムを示す．数十～数百個の高分子鎖が会合して疎水性の内核と親水性の外殻からなる球状構造を形成する．薬物は，B鎖に化学的に結合するか，B鎖が形成するミセル内核に物理的に封入される．

高分子ミセルが薬物キャリヤーとして有するおもな長所と短所を**表1**にまとめた(これ以外の項目については文献1)2)を参照されたい)．第一の長所は，10～100 nm の直径の超微粒子が容易に得られることである．一般的にこのサイズの範囲の微粒子を得ることは高度な技術が必要であるのに対し，高分子ミセルでは通常のことである．この範囲の粒径は，次項で述べる固形癌組織へのターゲティングで有用な大きさである．このことから，高分子ミセルは薬物キャリヤーのためのナノテクノロジーとして生来の利点を有していると言える．

第二の長所は，水に難溶性の薬物を封入することである．水に溶けない薬物は血液中に投与できないので，有毒な有機溶剤に溶かして血中に投与

〔キーワード〕
ターゲティング
EPR 効果
固形癌
高分子ミセル
DDS

* YOKOYAMA Masayuki/財団法人神奈川科学技術アカデミー

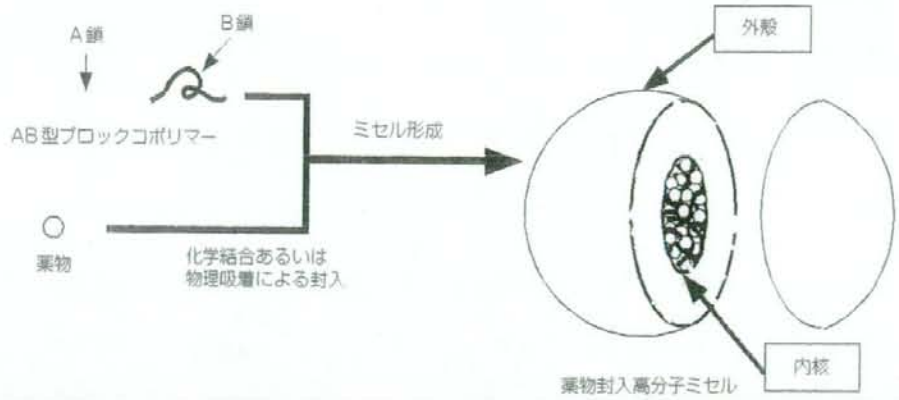

図 1. 高分子ミセル薬物キャリヤーシステムの構築

表 1. 薬物キャリヤーとしての高分子ミセルの長所と短所

長所
1，ナノ領域の超微粒子径が容易に得られる
2，水溶性に乏しい薬物封入に好適
3，生体への毒性が低い
短所
1，高分子材料の入手が容易でない
2，薬物の徐放化に高い技術が必要

するか，吸収の変動に妥協しても経口投与とするかの選択となるが，高分子ミセルを用いると容易に血液中投与が可能となる．海外では，ターゲティング能はもたないが，難溶性抗癌剤の可溶化に高分子ミセルを用いている例がある[3]．

第三の長所は生体内での毒性の低さである．これまで筆者がかかわった研究開発において，動物実験と臨床試験をとおしてキャリヤーシステムに基づくと考えられる副作用・毒性は見出されていない．このことが高分子ミセルは無毒ということではなく，抗癌剤の副作用(100%標的に運搬されないので抗癌剤の副作用は起こる)にくらべて無視できる程度であるということである．しかし，認可されたターゲティングシステムでは，元の抗癌剤にない意外な副作用が引き起こされたり，キャリヤーに基づく副作用を抑制するために，別の薬の前投与が必要になったりする場合がよく起こる[4][5]．よって，第三の長所の臨床的価値は決して低くない．

つぎに，高分子ミセル薬物キャリヤーとしての短所について述べてみたい．高分子ミセル特有の課題は，合成高分子としては珍しい部類のブロックコポリマーが必要なことである．とくに，ターゲティングを達成するには単にブロックコポリマーであるのみならず，その化学構造と鎖長が厳密に制御されて合成される必要がある[6]．また，高分子ミセルにかぎらずナノサイズのキャリヤーシステムで共通の問題は，キャリヤーがナノサイズであることによる，薬物の放出速度制御である．DDSの領域ではミクロンサイズのデバイスから薬物を徐放する研究開発は広範におこなわれてきた．薬物がキャリヤーから放出する機構は多くの場合，薬物分子の拡散であるので，キャリヤー(デバイス)が小さくなると格段にその制御が難しくなる．リポソームの場合には，薬物放出が速すぎるか，ほとんど放出しないかになりやすい．高分子ミセルの場合には，ミセル内核からの薬物放出速度の得られる幅が広いこと(数分から数十時間の時間スケールで)が特徴であるが，その速度をターゲティングに最適なものに制御するには，高分子構造の厳密な制御が必要である場合が多い．

2．高分子ミセルによる抗癌剤ターゲティングの現状

ここでまず，薬物ターゲティングの方式について短く解説したい．高分子ミセルを用いた固形癌へのターゲティングを理解するのに，必須な事柄であるからである．薬物ターゲティングは標的選択性を得る方式によって，アクティブターゲティングとパッシブターゲティングの2つの方法論に分類される[7]．第一の方法論の，アクティブターゲティング(active targeting)は標的との明確な特異的相互作用を利用してターゲティングをおこなう．具体的には抗体や磁性微粒子などをキャリヤーとする場合である．第二の方法論はパッシブターゲティング(passive targeting)で，これはキャリヤーの物理的・化学的な性質をうまく利用してデリバリーをおこなうものである．

高分子ミセルをキャリヤーに用いる場合には，パッシブターゲティングが基本になるが，どのようにして癌ターゲティングが可能になるのであろうか？　それは固形癌局所の組織学的，生理学的特性を巧みに利用することによる．癌組織では血管内皮の透過性は異常に亢進していると同時に，リンパ系による排出が抑制されているために，ナノサイズのキャリヤーは本質的に固形癌部位に選択的に蓄積する．これは EPR 効果(enhanced permeability and retention effect)とよばれ，1986年に前田，松村ら[8][9]によって提唱された．血管の透過性亢進現象は，炎症部位で一般的にみられる諸現象のうちの1つである．「癌は癒されることなき創傷」[10]と表現した Dvorak の有名な句は，炎症が癌組織1つの重要な性格であることを示している．

ここで，EPR 効果に基づいた固形癌ターゲティングを**図2**に示す．1986年の最初の論文では，EPR 効果は天然高分子のアルブミンを用いて示された．**図2A**に示すように，アルブミンが正常皮膚にくらべ固形癌に約10倍もの量が蓄積し，その高い濃度が長期間維持されていた．1986年以降，EPR 効果は天然高分子のみではなく，合成高分子[11]やリポソームなどの他のタイプのキャリヤーシステムにも適用できることが示されている．高分子ミセルの場合の例を**図2B**に示す．抗癌剤アドリアマイシンを高分子ミセルに封入することで，この抗癌剤を単独で投与したときにくらべて投与24時間後に，9倍ほどの量がマウス癌に到達していた．**図2A**と B では縦軸の意味も，くらべている対照も異なるのであるが，ターゲティングがない場合にくらべて10倍程度の量が24~48時間かけて癌に蓄積することは一致している．この一致は，キャリヤーシステムを適切に設計・作製すれば，EPR 効果に基づいたターゲティングが達成しうることを示している．

この結果を癌の化学療法の観点からみると，ある抗癌剤の効果が10倍にも増強しうることは驚異的なことである．ただし，**図2**の結果で注意しなければならないのは，これらは癌組織への送達量であって，抗癌活性と等価でないことである．等価でない理由は第一に，抗癌作用を発揮するためには癌組織内で，キャリヤーシステムから抗癌剤が放出して癌細胞に入る必要があるからである．理由の第二は，抗癌活性は癌細胞への殺細胞効果(薬物の主作用)と正常部位への副作用のバランスによって規定されるので，主作用と同様に副作用も増強すれば，トータルとしての抗癌活性は上がらないからである．幸いにも**図2B**の高分子ミセルの場合には抗癌活性も著しく上昇した．この事実は，上述した2つの点がこのシステムでは問題となっていなかったことを示す．

2007年9月現在では**表2**に示す4つの高分子ミセル製剤の臨床試験が進行中である[12]~[15]．シスプラチンと SN-38 のシステムは2006年に第 I 相を開始した．これらのうち，パクリタキセルを封入したシステムは臨床第 I 相試験を無事終了し，臨床第 II 相試験に進む予定であるとともに，4つの製剤のなかでは臨床試験を最も重点を置いて展

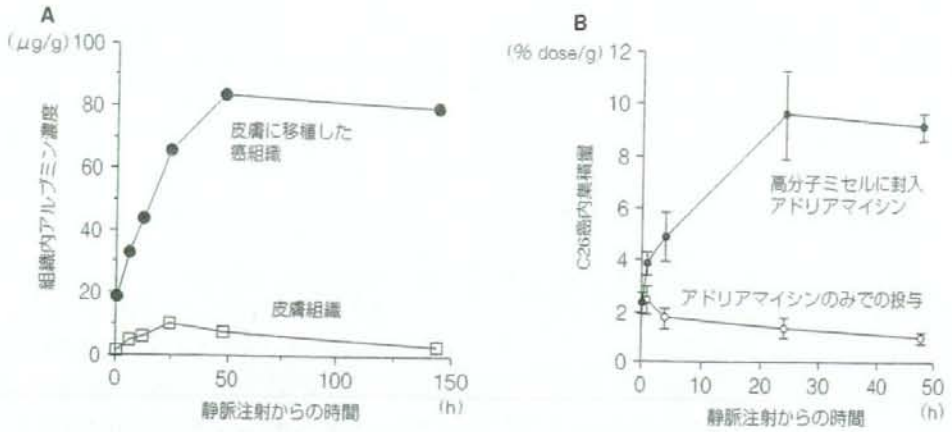

図 2. EPR 効果による固形癌へのターゲティング
A：アルブミンを用いた EPR 効果の実証(Matsumura Y *et al*, 1986[8]より筆者作成)
B：高分子ミセルによるターゲティング(Yokoyama M *et al*, *J Drug Targeting* **7**: 171-186, 1999 より筆者作成)

表 2. 臨床試験中の高分子ミセル抗癌剤

封入抗癌剤	臨床試験レベル	実施場所
アドリアマイシン	第Ⅱ相	日本(国立がんセンター)
パクリタキセル	第Ⅰ相終了	日本(国立がんセンター)
シスプラチン	第Ⅰ相	イギリス
SN-38(カンプトテシン誘導体)	第Ⅰ相	日本(国立がんセンター)

開してゆくものと位置づけられている.

おわりに
今後の発展方向

前項で述べたように，抗癌剤高分子ミセルシステムは臨床治験中であるので，4~5年後には評価が定まっているであろう．最後のこの項では，高分子ミセル薬物キャリヤーの今後の新たな発展方向を3つだけまとめたい．臨床的要素の高いものから基礎科学的なものの順番で述べてゆく．

まず第一の方向は，抗癌剤以外への展開である．抗癌剤が最初の応用例として選択された大きな理由の1つとして，キャリヤー自体の副作用の懸念がある．もし，この副作用が発生しても，抗癌剤の応用では相当な程度まで許容されるからである．幸いにも，上記の4つの抗癌剤としての臨床試験ではキャリヤー自体の副作用は見出されていない．正確なことは臨床試験の報告を待たねばならないが，抗癌剤よりも副作用が低い薬物への応用，より長期に投与する薬剤への応用が期待される．なかでも，固形癌組織との特徴を共有する炎症部位にはたらかせる薬物は，有力な候補と言える．

第二の発展方向は，画像診断への応用である．抗癌剤がターゲティングできるならば，造影剤をターゲティングすることによって癌診断を進歩させうると考えるのは自然なことである．この観点から筆者らは近年，高分子ミセル型MRI造影剤の研究に取り組んでいる．従来から，天然や合成高分子をMRI造影剤であるガドリニウム(Gd)イオンの癌特異的キャリヤーとして用いる研究はお

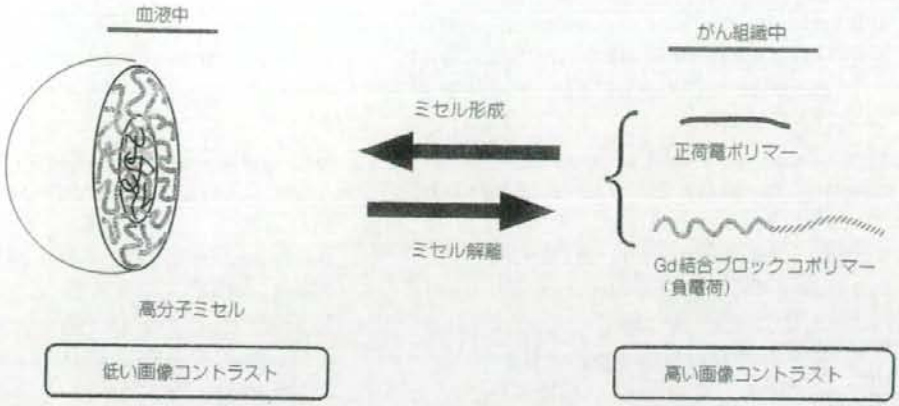

図 3. 高分子ミセル型 MRI 造影剤のアイデア

こなわれてきたが，抗癌剤のターゲティングにくらべて臨床的な応用は遅れているという現状である[16)~18)]．その理由の1つは，抗癌剤のデリバリーの場合と違って，造影剤の場合は血中濃度が高い状態であることが好ましくないことがある．上述した，EPR 効果を利用した癌組織ターゲティングでは，高い血中濃度を長時間保つことが必要条件となる．しかし，造影剤の場合には血液中にある造影剤は不要なバックグラウンドとして癌選択的画像の障害となりうる．血管は癌組織のみではなく正常組織にも通っているからである．

この問題の解決のために高分子ミセルの形成と解離現象を利用するのが，抗癌剤ターゲティングの場合にはなかった仕掛けである．**図3**に示すようにミセル構造形成によってミセル内に位置する Gd イオンが周囲の水分子から隔離されることで，T1 緩和時間短縮能(緩和能)を抑制する．ミセル形態で血液を循環しているあいだは，血液の画像コントラストは抑制される一方，癌組織内でミセル構造からブロックコポリマーに解離すると，Gd イオンは周囲の水に自由に接触することができ，T1 緩和能を発揮して癌組織をコントラスト高く映し出す．この高分子ミセルシステムは，*in vitro* でミセル構造の形成・解離によって約4倍の T1 緩和能の変化を得ることに成功した[19)]．今後は，*in vivo* でのターゲティングと癌選択画像取得に進んでゆくこととなる．

第三の発展方向は，薬物の封入と放出の制御である．この制御がある程度達成しているからこそ現状でもターゲティングできているのは事実であるが，まだ十分とは言えないのである．もともと，薬物をキャリヤーに封入あるいは結合することは，標的に到達するまでに薬効を示さない状態に保持することであり，標的での薬効発揮のための薬物放出とは反対の現象である．よって，薬物の保持と放出という相反する現象を，1つのキャリヤーシステムのなかで最適化することは技術的に難しい問題なのである．この問題に対して，技術的に最も明確な解決法は，癌選択的な薬物放出技術である．これらの技術はまだ基礎研究のレベルではあるが[20)]，次世代の技術として期待される．

文　献

1) Yokoyama M : Polymeric micelles as nano-sized drug carrier systems. In : *Nanoparticles for Pharmaceutical Applications*. ed by Domb AJ *et al*. American Scientific Publishers, Stevenson Ranch, 2007, pp. 63-72
2) Yokoyama M : Polymeric micelles for the targeting of hydrophobic drugs. In : *Polymeric Drug Delivery Systems*. ed by Kwon GS. Drug and Pharmaceutical Sciences, vol. 148. Taylor & Francis, 2005, pp. 533-575
3) Kim TY *et al* : Phase I and pharmacokinetic

study of Genexol-PM, a cremophor-free, polymeric micelle-formulated paclitaxel, in patients with advanced malignancies. *Clin Cancer Res* **10** : 3708-3716, 2004

4) Hamann PR *et al* : Mylotarg : The first antibody-targeted chemotherapy agant. In : *Tumor Targeting in Cancer Therapy*, ed by Page M. Humana Press, Totowa, 2002, pp. 239-254

5) Drummond DC *et al* : Liposomal drug delivery systems for cancer therapy. In : *Drug Delivery Systems in Cancer Therapy*, ed by Brwon DM. Humana Press, Totowa, 2004, pp. 191-213

6) Yamamoto T *et al* : What are determining factors for stable drug incorporation into polymeric micelle carriers? Consideration on physical and chemical characters of the micelle inner core. *J Control Release* **123** : 11-18, 2007

7) 高倉喜信ほか：パッシブターゲティングの意義. *Drug Delivery System* **14** : 425-426, 1999

8) Matsumura Y *et al* : A new concept for macromolecular therapeutics in cancer chemotherapy : Mechanism of tumoritropic accumulation of proteins and the antitumor agent smancs. *Cancer Res* **46** : 6387-6392, 1986

9) Maeda H *et al* : Advantages of macromolecular therapeutics *in vivo*. *Bioconjugate Chem* **3** : 351-361, 1992

10) Dvorak HF : Tumors : wounds that do not heal. Similarities between tumor stroma generation and wound healing. *N Engl J Med* **315** : 1650-1659, 1986

11) Seymour LW *et al* : Tumor tropism and anticancer efficacy of polymer-based doxorubicin prodrugs in the treatment of subcutaneous murine B16F10 melanoma. *Br J Cancer* **70** : 636-641, 1994

12) Matsumura Y *et al* : Phase I clinical trial and pharmacokinetic evaluation of NK911, a micelle-encapsulated doxorubicin. *Br J Cancer* **91** : 1775-1781, 2004

13) Hamaguchi T *et al* : NK105, a paclitaxel-incorporating micellar nanoparticle formulation, can extend *in vivo* antitumour activity and reduce the neurotoxicity of paclitaxel. *Br J Cancer* **92** : 1240-1246, 2005

14) Uchino H *et al* : Cisplatin-incorporating polymeric micelles (NC-6004) can reduce nephrotoxicity and neurotoxicity of cisplatin in rats. *Br J Cancer* **9** : 678-687, 2005

15) Koizumi F *et al* : Novel SN-38-incorporating polymeric micelles, NK012, eradicate vascular endothelial growth factor-secreting bulky tumors. *Cancer Res* **66** : 10048-10056, 2006

16) Rebizak R *et al* : Polymeric conjugates of Gd^{3+}-diethylenetriaminopentaacetic acid and dextran 1. Synthesis, characterization, and paramagnetic properties. *Bioconjug Chem* **8** : 605-610, 1997

17) Wang SC *et al* : Evaluation of Gd-DTPA-labelled dextran as an intravascular MR contrast agent : Imaging characteristics in normal rat tissues. *Radiology* **17** : 483-488, 1990

18) Bogdanov A *et al* : A long-circulating co-polymer in "passive targeting" to solid tumors. *J Drug Targeting* **4** : 321-330, 1997

19) Nakamura E : A polymeric micelle MRI contrast agent with changeable relaxivity. *J Control Release* **114** : 325-333, 2006

20) Nakayama M *et al* : Polymer terminal group effects on properties of thermoresponsive polymeric micelles with controlled outer-shell chain lengths. *Biomacromolecules* **6** : 2320-2327, 2005

Available online at www.sciencedirect.com
ScienceDirect
Journal of Controlled Release 126 (2008) 274–280
journal of controlled release
www.elsevier.com/locate/jconrel

Efficient peritoneal dissemination treatment obtained by an immunostimulatory phosphorothioate-type CpG DNA/cationic liposome complex in mice

Yukari Kuramoto, Shigeru Kawakami, Shuwen Zhou, Kyouichi Fukuda, Fumiyoshi Yamashita, Mitsuru Hashida *

Departments of Drug Delivery Research, Graduate School of Pharmaceutical Sciences, Kyoto University, Sakyo-ku, Kyoto 606-8501, Japan

Received 27 September 2007; accepted 7 December 2007
Available online 31 January 2008

Abstract

Peritoneal dissemination remains the most difficult type of metastasis to treat, and current systemic chemotherapy or radiotherapy tends to have little effect; therefore, immunotherapy using immunostimulatory CpG DNA could be a promising new therapeutic approach. Recently, we have reported that intraperitoneal administration of phosphodiester (PO) CpG DNA-lipoplex could efficiently inhibit peritoneal dissemination in mice. In this study, chemically modified phosphorothioate (PS)-CpG DNA and natural PO-CpG DNA were complexed with DOTMA/cholesterol cationic liposomes (PS-CpG DNA-lipoplex and PO-CpG DNA-lipoplex) and their antitumor activity was evaluated in a mouse model of peritoneal dissemination. Intraperitoneal administration of the PS-CpG DNA-lipoplex inhibited the proliferation of tumor cells in the greater omentum and the mesentery more efficiently than PO-CpG DNA-lipoplex. PS-CpG DNA-lipoplex induced higher cytokine production from primary cultured mouse peritoneal macrophages, suggesting that the high antitumor activity of the PS-CpG DNA-lipoplex is mediated by a high rate of cytokine production from immunocompetent cells such as macrophages. The serum transaminase levels of mice receiving intraperitoneal PS-CpG DNA-lipoplex treatment were measured to evaluate systemic toxicity, and these were found to be the same as those of untreated mice. These results suggest that intraperitoneal administration of PS-CpG DNA-lipoplex could be efficient immunotherapy for peritoneal dissemination.

Keywords: CpG DNA; Phosphorothioate; Peritoneal dissemination; Cationic liposome; Macrophage

1. Introduction

Peritoneal dissemination remains the most difficult type of metastasis to treat, and current systemic chemotherapy or radiotherapy tends to have little effect. The therapeutic problem of peritoneal dissemination is trans-lymphatic metastasis, that is, migration of the peritoneal free cancer cells through the lymphatic tissue, such as the milky spot on the greater omentum, spreading metastases throughout the body [1]. Since there are many immunocompetent cells in the lymphatic tissue, activation of these cells would be a new therapeutic strategy for peritoneal dissemination. It has been reported that CpG DNA, about 30-base oligonucleotides containing CpG dinucleotides, which is derived from the bacterial DNA, is recognized by Toll-like receptors (TLR)-9 expressed by macrophages and dendritic cells and induces Th1 type antitumor cytokines, such as tumor necrosis factor (TNF)-α and interleukin (IL)-12 [2,3]. Therefore, delivery of CpG DNA into lymphatic immunocompetent cells via the peritoneal cavity and induction of Th1 type cytokines in lymphatic tissues would effectively inhibit peritoneal dissemination.

As far as the molecular weight of the intraperitoneally injected compounds is concerned, a value of over 50,000 is required for efficient lymphatic organ distribution [4]. Since the molecular weight of naked CpG DNA is about 8000, intraperitoneally administrated naked CpG DNA cannot reach lymphatic organs. In fact, Agrawal et al. have reported that

* Corresponding author. Tel.: +81 75 753 4525; fax: +81 75 753 4575.
E-mail address: hashidam@pharm.kyoto-u.ac.jp (M. Hashida).

0168-3659/$ - see front matter © 2008 Elsevier B.V. All rights reserved.
doi:10.1016/j.jconrel.2007.12.007

intraperitoneally administered 20 mer naked oligonucleotide distributed into the blood and distributed in the kidney as well as intravenously administered oligonucleotide [5]. Since liposome-entrapped compounds are selectively distributed to the lymphatic organs following intraperitoneal administration [6,7], CpG DNA/cationic liposomes complex (lipoplex) formation is expected to enhance the distribution of CpG DNA to lymphatic organs. Recently, we have reported that intraperitoneal administration of phosphodiester (PO) CpG DNA-lipoplexes ranging in size from 100 to 200 nm could efficiently inhibit peritoneal dissemination in a mouse model [8].

In this study, we found that phosphorothioate (PS)-CpG DNA-lipoplex produced better therapeutic effects on peritoneal dissemination than PO-CpG DNA-lipoplex in mice. As far as the mechanism of the antitumor activity of the PS-CpG DNA-lipoplex was concerned, we also found that PS-CpG DNA-lipoplex resulted in significantly higher cytokine production than PO-CpG DNA-lipoplex after being taken up by macrophages. PS-CpG DNA-lipoplex or PO-CpG DNA-lipoplex were administered intraperitoneally using a peritoneal dissemination model in mice which involved the intraperitoneal inoculation of colon26/Luc cells, a mouse colorectal adenocarcinoma cell line that stably expresses firefly luciferase gene. We previously reported that some tumor cells are present in the lymphatic system (greater omentum) 24 h after intraperitoneal inoculation of tumor cells [9]. Therefore, in order to ensure the adhesion and invasion of the tumor cells in the lymphatic organs, PS-CpG DNA-lipoplex was administered 3 days after tumor cell inoculation. The numbers of tumor cells were quantitatively evaluated by measuring the luciferase activity in the greater omentum and the mesentery as the index of peritoneal dissemination [10,11]. In addition, TNF-α contributes to the antitumor activity and, therefore, the TNF-α produced by immunocompetent cells in response to TLR-9 activation was measured using the primary cultured mouse peritoneal macrophages.

2. Materials and methods

2.1. Animals

Male Balb/c (6-week-old) mice and female ICR (4-week-old) mice were purchased from the Shizuoka Agricultural Cooperative Association for Laboratory Animals (Shizuoka, Japan). Animals were maintained under conventional housing conditions. All animal experiments were approved by the Animal Experimentation Committee of the Graduate School of Pharmaceutical Sciences, Kyoto University.

2.2. Chemicals

RPMI1640 medium, phosphate buffered saline (PBS), Hanks' balanced salt solution (HBSS), and TGC medium were obtained from Nissui Pharmaceutical Co., Ltd. (Tokyo, Japan). Opti-MEM I was obtained from Invitrogen (Carlsbad, CA). Fetal bovine serum (FBS) was obtained from MP Biomedicals, Inc. (Irvine, CA). *N*-[1-(2,3-dioleyloxy)propyl]-*N*,*N*,*N*-trimethylammonium chloride (DOTMA) was purchased from Tokyo Chemical Industry, Co., Ltd. (Tokyo, Japan) and cholesterol was from Nacalai Tesque Inc. (Kyoto, Japan). Oligonucleotides with phosphorothioate and phosphodiester backbones were purchased from Operon (Tokyo, Japan). The sequences of the oligonucleotides were 5′-TCGACGTTTTG-ACGTTTTGACGTTTT-3′ (CpG DNA) and 5′-TGCAGCTT-TTGAGCTTTTGAGCTTTT-3′ (control GpC DNA). The level of TNF-α from the culture supernatant was determined by the ELISA Ready-SET-go! set (eBioscience, San Diego, CA). All other chemicals were of the highest grade available.

2.3. Preparation of liposomes and their complex with CpG DNA

Cationic liposomes were prepared as reported previously [12]. In brief, DOTMA and cholesterol were mixed in chloroform at a molar ratio of 1:1, then the mixture was dried, vacuum-desiccated, and resuspended in 5% dextrose solution in sterile test-tubes. After hydration for 30 min at room temperature, the dispersion was sonicated for 10 min in a bath sonicator, then for 3 min in a tip sonicator to form liposomes and, finally, sterilized by passing through a 0.45-μm filter (Nihon-Millipore Ltd., Tokyo, Japan). Liposome/CpG DNA complexes were prepared as described in previous reports [8]. An equal volume of stock liposome solution and CpG DNA in 5% dextrose were mixed at various charge ratios, and left at 37 °C for 30 min. The mean particle size and ζ-potential of the lipoplexes were measured using a Zetasizer nano ZS instrument (Malvern Instruments, UK).

2.4. Cell lines

Murine adenocarcinoma colon 26 tumor cells [13] was grown in 5% CO_2 in humidified air at 37 °C with RPMI1640 medium supplemented with 10% FBS, 100 IU/ml penicillin, 100 μg/ml streptomycin, and 2 mM L-glutamine. Colon26 cells that stably express the firefly luciferase gene (colon26/Luc) were established as previously reported [14,15].

2.5. Peritoneal dissemination model and the antitumor activity of the CpG DNA-lipoplex

Colon26/Luc cells were trypsinized, and the cell concentration was adjusted to 10^6 cells/ml in HBSS. Then, 0.1 ml of the cell suspension was inoculated intraperitoneally into male Balb/c mice. Three days after tumor inoculation, 5% dextrose, naked PS- and PO-CpG DNA (1 μg/mouse), PS- and PO-CpG DNA-lipoplex (1 μg/mouse at the charge ratio 3.1) were administered to the peritoneal cavity of mice (0.2 ml 5% dextrose solution/mouse). Ten days after tumor inoculation, the mice were euthanized by cervical dislocation and the greater omentum and mesentery were excised and washed with ice-cold saline. Then, the organs were homogenized in a lysis buffer (0.05% Triton X-100, 2 mmol/l EDTA, 0.1 mol/l Tris pH 7.8), and centrifuged at 10,000 g for 10 min. Ten microliter of the supernatant was mixed with 100 μl luciferase assay buffer (Picagene, Toyo Ink,

Tokyo Japan), and the light produced was measured in a luminometer (Lumat LB 9507, EG & G Berthold, Bad Wildbad, Germany). The luciferase activity of the peritoneal organs was converted to the number of colon26/Luc cells using a regression line as previously reported [8,15].

2.6. In vitro cytokine production from primary cultured peritoneal macrophages

Peritoneal macrophages from mice were cultured according to our previous report [16]. Briefly, peritoneal macrophages were obtained from ICR mice 6 days after intraperitoneal injection of 1 ml 3% thioglycollate medium. Collected macrophages were plated on 24-well culture plates at a density of 1×10^6 cells/ml and cultured for 24 h. Cells were washed with 0.5 ml PBS before use. The cells were incubated with Opti-MEM containing PS-CpG DNA-lipoplex, PO-CpG DNA-lipoplex, or PS-GpC DNA-lipoplex (5 μg DNA/ml) for 2 h, then, washed with PBS and incubated with Opti-MEM. Six or twenty-four after incubation, the supernatants were collected and ELISA used to determine TNF-α.

2.7. Evaluation of ALT and AST in serum after intraperitoneal administration of PS-CpG DNA-lipoplex

PS-CpG DNA-lipoplex (1 μg/mouse, charge ratio 3.1) was intraperitoneally administered to ICR mice. Blood was collected from the vena cava at 6, 24, and 48 h and allowed to coagulate for 8 h at 4 °C then serum was isolated as the supernatant fraction following centrifugation at 2000 g for 10 min. Serum ALT and AST were measured by the transaminase C II test Wako kit.

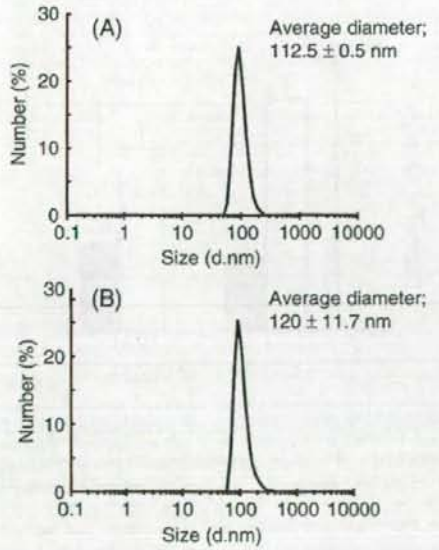

Fig. 1. Particle size distribution of (A) PS-CpG DNA-lipoplex and (B) PO-CpG DNA-lipoplex.

2.8. Statistical analysis

Statistical comparisons were performed by Student's t-test for two groups and one-way ANOVA for multiple groups. Post hoc multiple comparisons were made using Tukey's test. $P<0.05$ was considered significant.

3. Results

3.1. Particle size and ζ-potential of the PS-CpG DNA-lipoplex and PO-CpG DNA-lipoplex

To investigate the physicochemical properties of the PS-CpG DNA-lipoplex and PO-CpG DNA-lipoplex, their particle sizes and ζ-potential were determined. Both lipoplexes showed a clear-cut distribution pattern, and the mean particle size of the PS-CpG DNA-lipoplex (A) and the PO-CpG DNA-lipoplex (B) were 112.5±0.5 nm and 120±11.7 nm, respectively (Fig. 1). ζ-potential analysis showed that the ζ-potential of the PS-CpG DNA-lipoplex and the PO-CpG DNA-lipoplex were 53±0.2 mV and 52±0.3 mV, respectively ($n=3$). These results showed that there were no differences in terms of particle size and electric charge of the two lipoplexes.

3.2. Inhibition of peritoneal dissemination by intraperitoneal administration of PS-CpG DNA-lipoplex

The antitumor effects of the intraperitoneally administered PS-CpG DNA-lipoplex and the PO-CpG DNA-lipoplex on peritoneal dissemination were analyzed. Fig. 2 shows the number of tumor cells in the greater omentum (A) and the mesentery (B) after intraperitoneal administration of PS-CpG DNA-lipoplex and PO-CpG DNA-lipoplex at a DNA dose of 1 μg/mouse. In the PS-CpG DNA-lipoplex-treated group, the number of tumor cells in the greater omentum was about 9% compared with that of the PO-CpG DNA-lipoplex-treated group. The number of tumor cells in the mesentery of the PS-CpG DNA-lipoplex-treated mice was about 2% compared with that of the PO-CpG DNA-lipoplex-treated group. The number of tumor cells in the greater omentum (A) and the mesentery (B) after intraperitoneal administration at the DNA dose of 10 μg/mouse was also shown in Fig. 3. Intraperitoneal administration of PS-CpG DNA-lipoplex could reduce the numbers of tumor cells in both organs, and the number of tumor cells in the mesentery of the PS-CpG DNA-lipoplex-treated mice was significantly lower than that of PO-CpG DNA-lipoplex-treated mice.

3.3. Induction of TNF-α from primary cultured mouse peritoneal macrophages after treatment with PS-CpG DNA-lipoplex

As a mechanism of the antitumor activity of the PS-CpG DNA-lipoplex, the immunostimulatory effect of the PS-CpG DNA-lipoplex was evaluated using primary cultured mouse peritoneal macrophages. Primary cultured mouse peritoneal macrophages were treated with PS-CpG DNA-lipoplex and produced a higher level of TNF-α in the culture medium than

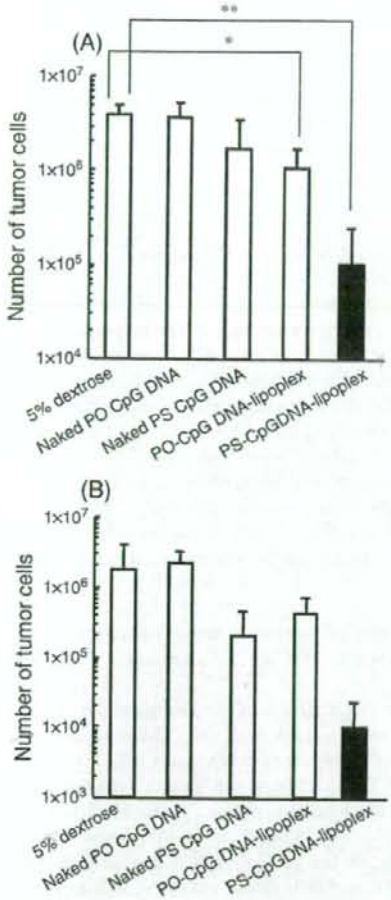

Fig. 2. The number of tumor cells in the (A) greater omentum and (B) mesentery of the peritoneal dissemination mice after intraperitoneal administration of PS-CpG DNA-lipoplex and PO-CpG DNA-lipoplex. Balb/c mice were intraperitoneally administered 5% dextrose, naked PS-CpG DNA, naked PO-CpG DNA, PS-CpG DNA-lipoplex and PO-CpG DNA-lipoplex after an intraperitoneal inoculation of colon26/Luc cells. Ten days after tumor inoculation, the luciferase activity of the greater omentum and the mesentery was measured and converted into the number of tumor cells. Results are expressed as mean+SD (n=4). *P<0.05, **P<0.01; The number of tumor cells was significantly different from 5% dextrose-treated group.

those treated with PO-CpG DNA-lipoplex (***P<0.001). On the other hand, PS-GpC DNA-lipoplex, which had no CpG motifs, did not induce any TNF-α production.

3.4. Evaluation of ALT and AST in serum after intraperitoneal administration of PS-CpG DNA-lipoplex

To evaluate the intraperitoneal administration of PS-CpG DNA-lipoplex, serum ALT and AST levels were measured. The ALT and AST levels in the serum of PS-CpG DNA-lipoplex-treated mice were the same as those of untreated mice (Fig. 5).

4. Discussion

To date, there are many reports about refractory peritoneal dissemination therapy using particle formation of chemotherapeutic agents with a low molecular weight based on enhancement of distribution in the lymphatic organs [4,17,18]. However, chemotherapy causes severe side-effects, therefore, immunotherapy would be a more promising approach.

The therapeutic problem associated with peritoneal dissemination is trans-lymphatic metastasis. As shown in Fig. 1, the particle size of both CpG DNA-lipoplexes was about 100 nm. These results suggest that both CpG DNA-lipoplexes could be more efficiently distributed to lymphatic organs than naked CpG DNA. In peritoneal dissemination model, PS-CpG DNA-lipoplex inhibited the proliferation of tumor cells more effectively compared with PO-CpG DNA-lipoplex after intraperitoneal administration (Figs. 2 and 3). High antitumor effects of

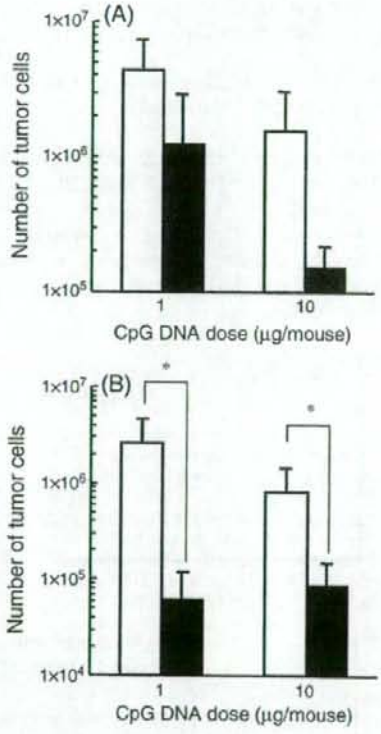

Fig. 3. Dose-dependent effect of intraperitoneally administered PS-CpG DNA-lipoplex and PO-CpG DNA-lipoplex in a mouse peritoneal dissemination model. Balb/c mice were intraperitoneally administered PS-CpG DNA-lipoplex (■) and PO-CpG DNA-lipoplex (□) at a dose of 1 μg or 10 μg DNA/mouse after an intraperitoneal inoculation of colon26/Luc cells. Ten days after tumor inoculation, the luciferase activity of the greater omentum (A) and the mesentery (B) was measured and converted into the number of tumor cells. Results are expressed as mean+SD (n=4). *P<0.05; The number of tumor cells of PS-CpG DNA-lipoplex-treated group was significantly different from PO-CpG DNA-lipoplex- treated group.

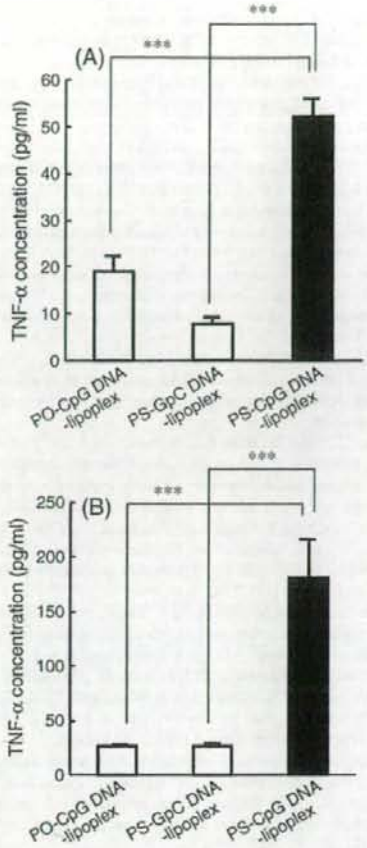

Fig. 4. TNF-α production from primary cultured mouse peritoneal macrophages after treatment with PS-CpG DNA-lipoplex. Primary cultured mouse peritoneal macrophages were treated with PS-CpG DNA-lipoplex, PO-CpG DNA-lipoplex, and PS-GpC DNA-lipoplex (no CpG motifs). The concentration of TNF-α in the culture medium after 6 h (A) and 24 h (B) incubation was determined by ELISA. Results are expressed as mean+SD (n=3). ***P<0.001; The TNF-α concentration of PS-CpG DNA-lipoplex treatment group was significantly different from PO-CpG DNA-lipoplex and PS-GpC DNA-lipoplex treatment group.

PS-CpG DNA-lipoplex might be mediated by the high immunostimulatory effect of PS-CpG DNA-lipoplex; therefore, TNF-α production was measured as an index of immunostimulation, using primary cultured mouse peritoneal macrophages. TNF-α production from PS-CpG DNA-lipoplex-treated cells was significantly higher than that from PO-CpG DNA-lipoplex (Fig. 4). Taking these findings consideration, the high antitumor effect of the PS-CpG DNA-lipoplex might be due to the potent immunostimulatory activity of the PS-CpG DNA-lipoplex after being taken up by immunostimulatory cells.

As far as the application of naked CpG DNA is concerned, PS modification has been widely used for protection from nuclease degradation. It has been found that peritumoral administration of naked PS-CpG DNA eradicated tumor growth by local induction of NK cells and $CD8^+$ T cells in solid tumor-bearing mice [19]. Another group have shown that intradermal administration of naked PS-CpG DNA around the tumor inhibits tumor growth and metastasis of melanoma cells [20]. In this study, naked PS-CpG DNA-lipoplex and PO-CpG DNA-lipoplex were intraperitoneally administered to treat peritoneal dissemination. However, as shown in Fig. 2, not only naked PO-CpG DNA but also naked PS-CpG DNA failed to inhibit the proliferation of tumor cells in the mouse peritoneal dissemination model. This lack of inhibition might be explained by the fact that the molecular weight of both naked CpG DNAs is about 8000, which is not high enough to distribute to the lymph organs after intraperitoneal administration [4].

For clinical application of intraperitoneal PS-CpG DNA-lipoplex, not only the efficacy but also the toxicity has to be considered. To date, there are many reports about the toxicity of systemic administration of plasmid DNA/cationic liposome complex (pDNA-lipoplex). Loisel S. et al. have reported that the main toxicity of systemically administered pDNA-lipoplex is observed in the liver and not the lung [21]. In this study, PS-CpG DNA-lipoplex was given intraperitoneally, however, if any intraperitoneally administered PS-CpG DNA-lipoplex was absorbed into the bloodstream, it might cause systemic toxicity. Therefore, the hepatic toxicity of intraperitoneally injected PS-CpG DNA-lipoplex was evaluated. As shown in Fig. 5, the serum ALT and AST levels of mice treated with PS-CpG DNA-

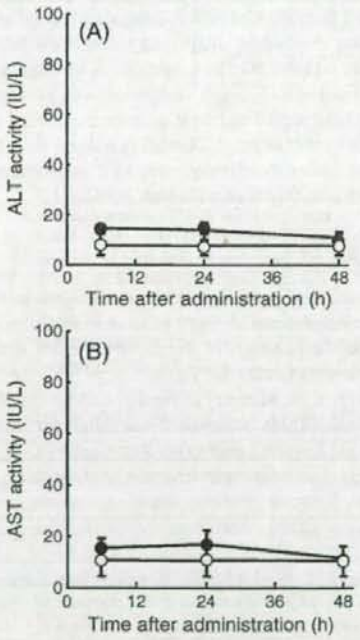

Fig. 5. Evaluation of hepatic toxicity after intraperitoneal administration of PS-CpG DNA-lipoplex. PS-CpG DNA-lipoplex (●) was administered to ICR mice. (○) represents the no treatment group. Serum ALT (A) and AST (B) levels 6, 24, and 48 h after administration were measured. Results are expressed as mean±SD (n=4).

lipoplex (1 μg DNA/mouse) were the same as those of untreated mice after intraperitoneal administration, suggesting that no hepatic toxicity was induced. These results for the hepatic toxicity correspond to an earlier report that the serum ALT level after intraperitoneal administration of pDNA-lipoplex (15 μg DNA/mouse) was within the normal range [22].

Recently, Edelatein et al. described the use of gene therapy in clinical trials [23]. According to the review, lipoplexes have already been used as a non-viral delivery vector. As far as the evaluation of the side effects of intraperitoneally administered lipoplex in clinical situations is concerned, Mudhusudan et al., have reported that no severe toxicity was observed at a DNA dose of 1.8 mg/m^2, and this DNA dose is equal to the dose of 15 μg/mouse [24]. In this study, we have demonstrated the potential use of PS-CpG DNA-lipoplex for therapeutic effects against peritoneal dissemination even at a DNA dose as low as 1 μg/mouse. Taking these findings into consideration, safe and effective peritoneal dissemination therapy using PS-CpG DNA-lipoplex could be used in clinical applications in the future.

It was also reported that CpG DNA reversed the immunosuppression state caused by chemotherapeutic agent [25,26]; therefore, combination of PS-CpG DNA-lipoplex and chemotherapy is expected to enhance the therapeutic effect against peritoneal dissemination by reversing the immunosuppressed state.

In conclusion, we have demonstrated that PS-CpG DNA-lipoplex exhibits more potent therapeutic effects on peritoneal dissemination than PO-CpG DNA-lipoplex after intraperitoneal administration in mice. A suggested mechanism for the antitumor activity of PS-CpG DNA-lipoplex is the higher cytokine production from macrophages compared with PO-CpG DNA-lipoplex. Although further investigations are needed to clarify the efficacy of this system in clinical practice, this information will be valuable for the development of immunotherapy treatments for refractory peritoneal dissemination.

Acknowledgements

This work was supported in part by Grants-in-Aid for Scientific Research from Ministry of Education, Culture, Sports, Science, and Technology of Japan, by Health and Labour Sciences Research Grants for Research on Advanced Medical Technology from the Ministry of Health, Labour and Welfare of Japan, by the Mochida Memorial Foundation for Medical and Pharmaceutical Research and by the 21st Century COE Program "Knowledge Information Infrastructure for Genome Science".

References

[1] Y. Yonemura, Y. Endo, T. Obata, T. Sasaki, Recent advances in the treatment of peritoneal dissemination of gastrointestinal cancers by nucleoside antimetabolites, Cancer Sci. 98 (1) (2007) 11–18.

[2] A.M. Krieg, A.-K. Yi, S. Matson, T.J. Waldschmidt, G.A. Bishop, R. Teasdale, G.A. Koretzky, D.M. Klinman, CpG motifs in bacterial DNA trigger direct B-cell activation, Nature 374 (6522) (1995) 546–549.

[3] H. Hemmi, O. Takeuchi, T. Kawai, T. Kaisho, S. Sato, H. Sanjo, M. Matsumoto, K. Hoshino, H. Wagner, K. Takeda, S. Akira, A toll-like receptor recognizes bacterial DNA, Nature 408 (6820) (2000) 740–745.

[4] K. Hirano, C.A. Hunt, Lymphatic transport of liposome-encapsulated agents: effects of liposome size following intraperitoneal administration, J. Pharm. Sci. 74 (9) (1985) 915–921.

[5] S. Agrawal, J. Temsamani, T.Y. Tang, Pharmacokinetics, biodistribution, and stability of oligodeoxynucleotide phosphorothioates in mice, Proc. Natl. Acad. Sci. USA 88 (1991) 7595–7599.

[6] R.J. Perker, K.D. Hertman, S.M. Sleber, Lymphatic absorption and tissue disposition of liposome-entrapped [^{14}C] adriamycin following intraperitoneal administration to rats, Cancer Res. 41 (4) (1981) 1311–1317.

[7] W.T. Phillips, L.A. Medina, R. Klipper, B. Goins, A novel approach for the increased delivery of pharmaceutical agents to peritoneum and associated lymph nodes, J. Pharmacol. Exp. Ther. 303 (1) (2002) 11–16.

[8] Y. Kuramoto, M. Nishikawa, K. Hyoudou, F. Yamashita, M. Hashida, Inhibition of peritoneal dissemination of tumor cells by single dosing of phosphodiester CpG oligonucleotide/cationic liposome complex, J. Control. Release 115 (2) (2006) 226–233.

[9] K. Hyoudou, M. Nishikawa, Y. Kobayashi, Y. Kuramoto, F. Yamashita, M. Hashida, Inhibition of adhesion and proliferation of peritoneally disseminated tumor cells by pegylated catalase, Clin. Exp. Metastasis 23 (5–6) (2006) 269–278.

[10] Y. Ikehara, T. Niwa, L. Biao, S.K. Ikehara, N. Ohashi, T. Kobayashi, Y. Shimizu, N. Kojima, H. Nakanishi, A carbohydrate recognition-based drug delivery and controlled release system using intraperitoneal macrophages as a cellular vehicle, Cancer Res. 66 (17) (2006) 8740–8748.

[11] M.J. Lee, S.S. Cho, J.R. You, Y. Lee, B.D. Kang, J.S. Choi, J.W. Park, Y.L. Suh, J.A. Kim, D.K. Kim, J.S. Park, Intraperitoneal gene delivery mediated by a novel cationic liposome in a peritoneal disseminated ovarian cancer model, Gene Ther. 9 (13) (2002) 859–866.

[12] S. Kawakami, A. Sato, M. Nishikawa, F. Yamashita, M. Hashida, Mannose receptor-mediated gene transfer into macrophages using novel mannosylated cationic liposomes, Gene Ther. 7 (4) (2000) 292–299.

[13] T.H. Corbett, D.P. Griswold Jr., B.J. Roberts, J.C. Peckham, F.M. Schabel Jr., Tumor induction relationships in development of transplantable cancers of the colon in mice for chemotherapy assays, with a note on carcinogen structure, Cancer Res. 35 (1975) 2434–2439.

[14] K. Hyoudou, M. Nishikawa, Y. Umeyama, Y. Kobayashi, F. Yamashita, M. Hashida, Inhibition of metastatic tumor growth in mouse lung by repeated administration of polyethylene glycol-conjugated catalase: quantitative analysis with firefly luciferase-expressing melanoma cells, Clin. Cancer Res. 10 (22) (2004) 7685–7691.

[15] K. Hyoudou, M. Nishikawa, Y. Kobayashi, Y. Kuramoto, F. Yamashita, M. Hashida, Inhibition of adhesion and proliferation of peritoneally disseminated tumor cells by pegylated catalase, Clin. Exp. Metastasis 23 (5–6) (2006) 269–278.

[16] T. Takagi, M. Hashiguchi, R.I. Mahato, H. Tokuda, Y. Takakura, M. Hashida, Involvement of specific mechanism in plasmid DNA uptake by mouse peritoneal macrophages, Biochem. Biophys. Res. Commun. 245 (3) (1998) 729–733.

[17] Y. Sadzuka, S. Hirota, T. Sonobe, Intraperitoneal administration of doxorubicin encapsulating liposomes against peritoneal dissemination, Toxicol. Lett. 116 (2000) 51–59.

[18] C.L. Zavaleta, W.T. Phillips, A. Soundararajan, B.A. Goins, Use of avidin/biotin-liposome system for enhanced peritoneal drug delivery in an ovarian cancer model, Int. J. Pharm. 337 (1–2) (2007) 316–328.

[19] Y. Kawarada, R. Ganss, N. Garbi, T. Sacher, B. Arnold, G.J. Hammerling, NK- and CD8$^+$ T cell-mediated eradication of established tumors by peritumoral injection of CpG-containing oligodeoxynucleotides, J. Immunol. 167 (9) (2001) 5247–5253.

[20] N. Kuninaka, K. Sano, M. Honda, I. Kuniaki, J. Matsunaga, R. Okuyama, K. Takahashi, H. Watanabe, G. Tamura, H. Tagami, T. Terui, Peritumoral CpG oligodeoxynucleotide treatment inhibits tumor growth and metastasis of B16F10 melanoma cells, J. Invest. Dermatol. 123 (2) (2004) 395–402.

[21] S. Loisel, C.L. Gall, L. Doucet, C. Ferec, V. Flock, Contribution on plasmid DNA to hepatotoxicity after systemic administration of lipoplexes, Hum. Gene Ther. 12 (6) (2001) 685–696.

[22] X. Xing, L. Liu, W. Xia, L.C. Stephens, L. Huang, G. Lopez-Berestein, M.-C. Hung, Safety studies of the intraperitoneal injection of E1A-liposome complex in mice, Gene Ther. 4 (3) (1997) 238–243.